

NATIONAL ADVISORY COMMITTEE FOR AERONAUTICS

WARTIME REPORT

ORIGINALLY ISSUED

August 1943 as
Advance Restricted Report 3H24

DEVELOPMENT OF THERMAL ICE-PREVENTION EQUIPMENT
FOR THE B-17F AIRPLANE

By Alun R. Jones and Lewis A. Rodert

Ames Aeronautical Laboratory
Moffett Field, California



WASHINGTON

NACA WARTIME REPORTS are reprints of papers originally issued to provide rapid distribution of advance research results to an authorized group requiring them for the war effort. They were previously held under a security status but are now unclassified. Some of these reports were not technically edited. All have been reproduced without change in order to expedite general distribution.

NATIONAL ADVISORY COMMITTEE FOR AERONAUTICS

ADVANCE RESTRICTED REPORT

DEVELOPMENT OF THERMAL ICE-PREVENTION EQUIPMENT FOR THE B-17F AIRPLANE

By Alun R. Jones and Lewis A. Rodert

SUMMARY

A thermal ice-prevention system for the B-17F airplane has been developed at the Ames Aeronautical Laboratory of the National Advisory Committee for Aeronautics in cooperation with the Materiel Command of the Army Air Forces, and the Boeing Aircraft Company. The report includes a description of the design, an outline of the design analysis, and a presentation and discussion of flight-test thermal data secured under non-icing conditions. Performance of the system under natural icing conditions is to be presented in a supplementary report.

The basic idea in the design of the system described was to raise the temperature of the surfaces to be protected from ice formations by subjecting the inner faces to a stream of heated air. The sources of heated air were three exhaust-gas-to-air heat exchangers: one located in each outboard nacelle, and the third located in the right inboard nacelle. A double-skin type of construction was employed over the forward portion of the wings and tail surfaces. The heated air was caused to circulate by the dynamic pressure of the air stream.

The design analysis was based upon a procedure developed by the AAL. The critical design data which apply to the B-17F airplane installation, and their method of calculation, are presented.

Sufficient instrumentation was provided in the installation to allow for determination of the heat flow throughout the system. Tables are presented of the temperatures of the heated circulating air and surfaces, and the capacity of the heat exchangers, in flights at 10,000 and 18,000 feet pressure altitude. Curves are presented showing the exhaust gas and circulating air-pressure drops for one of the exchangers, based upon investigations in flight with the

exchanger installed upon a single-engine test airplane.

The test data indicate that the thermal ice-prevention system removes, from the exhaust gas, about 10 percent of the heat available above free-air temperature. Based upon experience gained with previous thermal ice-prevention installations, in flight under natural icing conditions, the heat flow in the system is sufficient to provide satisfactory ice protection for the wing outer panels, but may be inadequate for the empennage and wing tips.

INTRODUCTION

In cooperation with the Materiel Command of the Army Air Forces, the Boeing Aircraft Company, and several equipment manufacturing companies, the AAL has designed, installed, and tested in flight a thermal ice-prevention system for the B-17F airplane. The work was undertaken at the request of the Materiel Command, for whom the AAL had previously designed and tested several thermal ice-prevention systems on a Lockheed 12A airplane (reference 1) and one system on a Consolidated B-24D airplane (reference 2). Appreciation is extended to representatives of the Boeing Aircraft Company, Messrs. Roy Ostling and John Riley, who contributed valuable experience to the development of the project.

DESCRIPTION OF THE ICE-PREVENTION EQUIPMENT

The B-17F airplane is shown in figure 1. The airplane is a midwing monoplane of the heavy bombardment type, powered by four Wright model R-1820-97 engines, having a sea-level rating of 1000 horsepower. Each engine is equipped with an exhaust-driven type B-2 turbosupercharger.

The general layout of the thermal ice-prevention system for the B-17F airplane is shown in figure 2. Heated air is obtained from exhaust-gas-to-air heat exchangers in nacelles 1, 3, and 4 and directed to the regions to be heated by a system of thin-wall, aluminum-alloy ducts.

The design of the equipment for the wing outer-panel leading edge from stations 19A to 33 is shown in figure 3. The flow of the heated air is directed along the inner

face of the airfoil skin in a chordwise direction by corrugated sheets attached to the outer skin. These sheets extend from rib to rib and consist of upper and lower portions, separated at the leading edge to provide an opening for the heated air to enter the chordwise passages. Both portions terminate at approximately 15 percent of the wing chord. Distribution of the heated air to the chordwise passages is obtained by means of a spanwise bulkhead placed at 4 percent of the wing chord. All of the heated air for the outer panel is delivered to the single spanwise duct at its inboard end, in contrast to the multi-duct supply system employed in the B-24D design of reference 2. The truss structure of the front spar allows the air to pass into the wing interior, and from there it is discharged through the aileron slot. The outer-panel leading edge during revisions, before the 4-percent-chord bulkhead was installed, is shown in figure 4, and the completed leading edge as viewed from the rear is shown in figure 5.

The design of the wing-tip ice-prevention installation is shown in figure 6. The spanwise duct is terminated at the tip joint by a solid wing rib web. The heated air for the wing tip, therefore, is obtained from the interior of the wing outer panel and has flowed through the chordwise passages.

The carburetor and intercooler air inlets are located in the wing leading edge near the nacelles, two inlets being provided for each engine. In installations of this type, there is a tendency for ice to accumulate on the edges of these inlets, particularly the lower lip. Because protection for all edges was unpracticable, an experimental installation was provided for the lower lips only of the intakes for the right outboard engine. Heated air is supplied to the surfaces to be protected by a 1-inch branch from the supply duct to the wing outer-panel leading edge (fig. 7). Flattened outlets cause the heated air to impinge on the lower edges of the intake openings.

The thermal ice-prevention design for the wing inboard panel (stations 8, 9, and 10) is shown in figure 8. A portion of the heated air from the exchanger in nacelle 3 is diverted to the inboard panel leading edge, as shown in figure 2, and enters a semicircular spanwise duct located on the lower surface of the wing. At the forward edge of the spanwise distribution duct, the air enters a narrow passage, formed between the inner and outer skins, which is continuous around the leading edge. The gap between

the two skins is 1/16-inch and extends over the forward 4 percent of the leading edge, top and bottom. The air is discharged into the wing interior at the gap outlet on the upper surface. The left wing leading edge was revised in the same manner as the right wing, but was not connected to a supply of heated air, pending the possible installation of a heat exchanger in nacelle 2.

The primary function of the heat exchanger in nacelle 3 is to furnish heated air for the empennage. The supply duct from nacelle 3 to the empennage is indicated in figure 2. Portions of the duct inside the right wing, and inside the fuselage, are shown in figures 9 and 10. The entire duct line from the nacelle to the empennage was insulated with a 1-inch thick blanket of rock-wool type material and covered with linen cloth.

Details of the fin and dorsal thermal ice-prevention system are shown in figure 11. Considering first the dorsal heating system, heated air is carried to the leading edge in a 3-inch bypass from the main empennage duct. This air is directed into a passage formed by the dorsal leading-edge inner skin and a baffle located about 6 inches from the leading edge. The heated air leaves the passage through holes in the leading edge of the inner skin and flows through the 0.06-inch gap between the outer and inner skins.

The fin leading edge is heated in a manner identical to that described for the dorsal. Heated air for the leading-edge system is supplied by a 3-inch duct located just aft of the joint between the dorsal and vertical fin. A portion of the leading edge, typical for both fin and dorsal, is shown in figures 12 and 13.

The ice-prevention equipment for the horizontal stabilizer is shown in figure 14. A single 3-inch supply duct to each stabilizer branches into three leading-edge ducts. The stabilizer leading edge was not removable, and the somewhat complicated system of ducts shown in figure 14 was required to obtain a satisfactory temperature distribution without redesigning the leading edge.

The heated air in the leading-edge ducts passes through slots located on the forward face of the ducts, through holes in the nose inner skin, and through a 0.05-inch gap between the inner and outer skins. Flow of the air to the interior of the stabilizer is prevented by a

spanwise bulkhead aft of the slotted tubes. Details of the stabilizer ice-prevention installation are shown in figures 15 and 16. For the entire empennage design, the outer skin of the leading edge covers approximately the same surface area as that originally occupied by the rubber de-icers.

To facilitate the heat-exchanger design, a removable portion of the exhaust stack between the collector ring and the turbosupercharger was modified to give more heat-transfer area. The altered exhaust stack for one of the outboard nacelles is shown in figure 17. The main shell and inner fins consist of a single sheet of stabilized stainless steel, folded longitudinally to form the inner fins and welded at the seam and fin ends. The outer fins are formed by cutting slots in 2-inch wide by 0.040-inch thick copper strips. The slots are 1/16-inch wide and are spaced to provide for fins 1/8-inch wide. The solid portion of the strips was inserted between the folds forming the inner fins and was furnace-brazed to the stainless steel. The outer fins were then twisted 90° so that the direction of the 1/8-inch dimension would coincide with that of the air flow. The asbestos cloth seals shown at the ends of the exchanger in figure 17 are designed to fit against the exhaust-stack shroud and prevent air leakage.

The heat exchanger air-intake scoops are attached to the sides of the nacelles as shown in figure 18 for the right inboard nacelle and figure 19 for the outboard nacelles. For later flight tests under natural icing conditions, the intake lips were heated with warm air taken from behind the cowl flaps.

The heated-air outlet from the exchanger in the right outboard nacelle is shown in figure 20. An overboard dump system is provided by the installation of a plate valve inside the main duct which can divert the air out through the rectangular opening shown in the figure. A removable duct section is attached to the flange of the rectangular outlet, and the air is dumped as shown in figure 21. The installation of the dump-valve drive motor for the right outboard nacelle is shown in figure 22. The heated-air outlet and dump valve for the exchanger in the right inboard nacelle are shown in figure 23. The valve drive motor installation is shown in figure 24.

A separate switch for each dump-valve drive motor is installed on the pilot's instrument panel (fig. 25). These switches are of the toggle, snap-position type, and the motor is stopped at the extremes of the valve travel by limit contacts in the circuit. An iron-constantan thermocouple is installed in each exchanger outlet and is connected to a selector switch, which in turn is connected to a temperature indicator (fig. 25). A zinc-strip safety device is also installed in each exchanger outlet. Should leakage of exhaust gas into the air side of the heat exchanger cause the air temperature to exceed 800° F, the zinc strip is melted and a warning light is operated.

The distribution of the heated air from the right inboard exchanger is controlled by means of nine butterfly valves in the system, located as shown in figure 2. The valves are not adjustable in flight; therefore, the settings for the desired distribution were determined in preliminary flight tests, and the valves were fixed at these positions.

Design Analysis of Thermal Ice-Prevention Equipment

The design analysis procedure for the B-17F airplane was almost identical to that outlined for the B-24D airplane in reference 2. The results of the analysis, and a condensation of the step-by-step procedure of reference 2 as applied to the wing outer panel, are presented in this report. The nomenclature is the same as that listed in reference 2.

For purposes of design, an indicated airspeed of 155 miles per hour and a pressure altitude of 18,000 feet were assumed.

Step 1. Assumption of free air temperature.- A free air temperature of 0° F was assumed.

Step 2. Assumption of average temperature at which the heated surface is to be maintained.- An average temperature rise of 90° F was assumed for the wing outer-panel surface to which direct heating could be applied. In the case of the B-17F airplane, direct heating was applied to the forward 15 percent of the wing chord, as compared with 10 percent of the chord for the B-24D airplane.

Step 3. Calculation of the heat-transfer coefficient between the wing surface and the ambient air.- The heat-transfer coefficient h was calculated by equation (1) of reference 2. The effect of change in altitude upon the value of the transfer coefficient has been neglected in the equation. The heat-transfer coefficients for the leading edge as calculated by equation (1) of reference 2 are plotted in figure 26.

Step 4. Calculation of the total heat flow from the critical design surface.- The heat removed from the leading edge outer surface was calculated by equation (2) of reference 2. The value of s for the wing leading edge forward of the front spar is plotted in figure 26. The average values of h and s from figure 26 are 15.5 Btu per hour, square foot, $^{\circ}\text{F}$, and 3.9 feet, respectively. From equation (2) of reference 2, the heat flow from the leading edge:

$$Q_{6-7} = (h_{6-7})_{av} S (t_{6-7})_{av} = \frac{15.5 \times 211 \times 3.9 \times 90}{12}$$

$$Q_{6-7} = 95,000 \text{ Btu per hour}$$

Step 5. Estimate of the required heat capacity for the circulating air.- As stated in reference 2, the quantity of heat supplied to the leading-edge system in the circulating air is usually taken as two to four times the amount of heat transferred through the leading-edge outer surface. For the B-17F design, a value of two to two and one-half times the quantity of heat calculated in step 4 was considered sufficient. The design capacity for the outboard heat exchangers was approximately established at between 190,000 and 240,000 Btu per hour.

Step 6. Calculation or assumption of air-flow rate through heat exchanger.- The B-17F exchangers are almost identical to those employed in the B-24D airplane, and for design purposes the air-flow rate was assumed to be the same, or 2730 pounds per hour.

Step 7. Calculation of heat-exchanger capacity and air temperature rise.- Heat-exchanger dimensions which previous experience had indicated would satisfy the requirements of steps 5 and 6, and would provide a temperature rise

of approximately 300° F, were assumed. The exchanger performance was then calculated. The resulting heat output was 213,000 Btu per hour, with a temperature rise of 320° F. The quantity of heat supplied to the wing interior aft of 15-percent chord then becomes 213,000 minus 95,000, or 118,000 Btu per hour.

Step 8. Design of the heated-air passages.— The use of the B-24D type corrugations in the B-17F design was considered desirable from a production standpoint. With the corrugation size and the air-flow rate fixed, the design problem was reduced to the determination of the outer-surface temperature produced by these conditions. The heat flow from a single chordwise passage, at several spanwise locations, was investigated.

Step 9. Application of steps 2, 3, and 4 to individual chordwise strips.— The heat flow from a single chordwise passage at any station is given by equation (4) of reference 2 as:

$$q_{6-7} = h_{6-7} t_{6-7} \frac{s}{12}$$

For the B-17F wing outer panel at station 19,

$$h_{6-7} = 14.1 \quad t_{6-7} = 90^{\circ} \text{ F} \quad s = 4.75 \text{ feet}$$

and therefore,

$$q_{6-7} = 502 \text{ Btu per hour per corrugation}$$

Step 10. Assumption of weight distribution of heated air.— The weight distribution of the heated air along the span was assumed the same as for the B-24D design (equation (5), reference 2).

$$w = w_{av} \sqrt{\frac{s_{av}}{s}}$$

The value of w at station 19 then becomes:

$$w = \frac{2730}{2 \times 211} \sqrt{\frac{3.88}{4.75}} = 5.85 \text{ pounds per hour}$$

Note that w is the actual air flow in a single upper or lower chordwise passage and therefore equals one-half the flow per corrugation.

Step 11. Calculation of the temperature drop of the heated air in the chordwise passages.— The temperature drop is determined by an adaptation of equation (3) of reference 2. For the air in a single passage at station 19:

$$t_1 - t_3 = \frac{q_{s-7}}{2 c_p w} = \frac{502}{2 \times 0.244 \times 5.85} = 176^\circ \text{ F}$$

Assuming the heated air enters the passage with temperature $t = 320^\circ \text{ F}$, the average temperature in the passage,

$$t_{2 \text{ av}} = 320 - \frac{176}{2} = 232^\circ \text{ F}$$

Step 12. Design of the heated-air passage to produce the required heat flow.— The method employed to calculate the heat-transfer coefficient for the inner surface of the wing for the B-17F was identical to that used for the B-24D. For the corrugation at station 19:

$$G = \frac{w}{A} = \frac{5.85}{3600 \times 0.000765} = 2.13 \text{ pounds per second, square feet}$$

$$Re = \frac{G D_e}{\mu} = \frac{2.13 \times 0.0172 \times 10^5}{1.47} = 2490$$

$$\frac{h_{2-s} D_e}{k} = 10.5 \quad (\text{curve AA, fig. 22, reference 2})$$

$$h_{2-s} = \frac{0.0159 \times 10.5}{0.0172} = 9.66 \text{ Btu per hour, square feet, } ^\circ \text{ F}$$

The average temperature in the air passage being 232° F , the available heat flow to the outer skin per corrugation becomes:

$$\begin{aligned}
 q_{2-6} &= h_{2-6} \times \frac{s}{12} \times (t_{2_{av}} - t_e) \\
 &= 9.66 \times \frac{4.75}{12} (232 - 90) \\
 &= 544 \text{ Btu per hour per corrugation}
 \end{aligned}$$

The calculated rates of heat flow per corrugation of 544 Btu per hour to the outer surface, and 502 Btu per hour from the outer surface, are in satisfactory agreement. The analysis for the remainder of the wing outer-panel leading edge was completed by the method just outlined, and the results are presented in figure 27.

The analysis procedure for the empennage was similar to that employed for the wings. The heat-transfer coefficients for the outer surface of the leading-edge skin of the horizontal stabilizer were calculated by equation (1) of reference 2, and are presented in figure 28. The heat-transfer coefficients for the dorsal and fin leading edges were not calculated, an average value of 12 Btu per hour per square foot per °F being assumed. The heated air at a total flow rate of 2700 pounds per hour was assumed to reach the empennage at a temperature of 250° F.

The values of $\frac{h D_e}{k}$ corresponding to the curve for air flow in narrow gaps from figure 22 of reference 2, were used in determining the heat-transfer coefficient for the inner surface of the outer skin. In using this curve, Reynolds number was based upon d (the gap width) rather than $2d$ (the gap hydraulic radius for 1 ft of span).

The results of the analysis for the stabilizer are presented in figure 29, and for the dorsal and fin, in figure 30. The analysis showed a required heat flow of 62,000 Btu per hour to each side of the stabilizer and 38,500 Btu per hour to the dorsal and fin. Based upon an assumed 320° F temperature rise in the right inboard heat exchanger, the design capacity of the exchanger became approximately 208,000 Btu per hour.

The pressure drop in the heated-air passages and the supply ducts was calculated by equation (6) of reference 2, which is written:

$$P_1 - P_2 = \frac{G^2 (v_2 - v_1)}{g} + \frac{f_{av} N G^2 v_{av}}{2gm}$$

The value of the friction factor f was obtained from figure 24 of reference 2. In the case of the chordwise passages, Reynolds number was based upon the equivalent diameter (four times the hydraulic radius), and the curve for laminar flow in pipes was used. In the case of the empennage gaps, Reynolds number was based upon the gap width d , and the curve for flow in narrow gaps was used. To estimate the pressure drop in the spanwise duct of the wing outer panel, the drop per foot was calculated for several points along the span and plotted as shown in figure 31. The average value was multiplied by the duct length to obtain the total, 0.3 inch of water (fig. 27). This pressure drop was considered negligible when compared to that in the chordwise passages and, therefore, no extra supply ducts to the leading edge (as required for the B-24D) were included in the B-17F design. The calculated pressure drops for the empennage gaps are shown in figures 29 and 30.

Instrumentation of the B-17F Airplane for Tests

Thermocouples, pressure orifices, and venturi meters were included in the design of a portion of the B-17F airplane thermal ice-prevention equipment in order to measure the performance of the installation in flight tests. The following factors were considered to be of interest:

- (1) Quantity of air flow through the heat exchangers
- (2) Temperatures of the heated air throughout the system
- (3) Temperatures of the heated surfaces: namely, wing and empennage outer surfaces and several points on the internal structure
- (4) Temperature of the exhaust gas

Consideration was given to measuring the exhaust gas and air-pressure drops across the heat exchangers, but the ducting installations did not lend themselves readily to such measurements. Satisfactory data for the right inboard exchanger, however, were obtained when the exchanger was installed on a single-engine test airplane with ducting

very similar to the B-17F installation. These data are presented in figure 32. The pressure drops in figure 32 correspond to the actual difference in static pressures measured at the exchanger inlet and outlet, in ducts of equal cross-sectional area.

The air flow through the exchangers was measured with venturi meters; one installed in the 5-inch supply duct to the wing outer panel, and the other in the 6-inch supply line to empennage (fig. 2). The 6-inch venturi meter could not be located between the exchanger outlet and the bypass to the wing inner panel because of installation difficulties. The air-flow rate obtained with this meter, therefore, was not an exact measurement of the flow through the exchanger, and the exchanger capacities based upon this flow rate are slightly slightly conservative. The deviation from the true exchanger capacity was not considered to be of sufficient magnitude to warrant additions to the instrumentation. The locations of the venturi-meter pressure orifices are shown in figure 33. The pressure drops at the venturi meters were obtained with a water manometer. The meters were calibrated before installation.

All temperatures were measured with iron-constantan thermocouples and a Lewis potentiometer. An identification drawing for the thermocouple locations is presented in figure 33. The dash numbers following the thermocouple numbers refer to the type of thermocouple mounting as detailed in figure 34.

TEST RESULTS AND DISCUSSION

Five flights were made to test the performance of the thermal ice-prevention equipment. During the first three flights, adjustments were made in the heated-air supply lines by means of the butterfly valves in order to obtain a satisfactory temperature distribution over the heated surfaces. Two more flights were then conducted to secure complete thermal data; one at 10,000 feet, and the other at 18,000 feet pressure altitude. The test data from these last two flights are presented in tables I, II, and III. The thermocouple and pressure-orifice designations correspond to those shown in figure 33.

The data from table II, flight 2, indicate that an average temperature rise of approximately 100° F was obtained over the forward 15 percent of the wing outer-panel

leading edge for an air-flow rate of 71 percent, and a heat-exchanger capacity of 86 percent, of the design figures. The temperature rise over the first 5 percent of the chord was considerably higher than the rise from 10- to 15-percent chord. Although the design features of the outer panel expose the foremost part of the airfoil to the warmest air, at least a part of the large temperature drop experienced at about 5-percent chord is believed to be caused by transition from laminar to turbulent flow occurring in that locality. An approximation of the heat flow through the skin over the wing outer panel forward of 15-percent chord was obtained by calculating the average air-temperature drop through the chordwise passages from the flight-test data. The total heat flow was 85,000 Btu per hour for flight 1, and 88,000 Btu per hour for flight 2, or approximately 50 percent of the heat supplied to the leading-edge system. This is equivalent to about 1250 Btu per hour per square foot of wing leading-edge surface. These figures for total heat flow are in good agreement with the design figure of 95,000 Btu per hour; however, attention is directed to the fact that the test data do not allow accurate determination, and the agreement is fortuitous.

Approximately 184,000 Btu per hour (72 hp) was extracted from the exhaust gas in each outboard engine, or about 10 percent of the heat available (above free-air temp.) in the gas.

A considerable temperature gradient was observed around the inboard section leading edge (table III). A more even temperature distribution could be obtained by increasing the gap size, or if necessary, tapering the gap. Because the system may be satisfactory in its present form, these changes were not made pending further tests.

The data from table III also indicate that the temperature rises of the dorsal, fin, and stabilizer leading edges are below design values, but not to a serious degree. Whether or not the surfaces have been heated sufficiently to provide satisfactory ice protection can only be determined by flights in natural icing conditions, but present available information suggests that only minor alterations, if any, will be required.

The capacity of the exchanger in the right inboard nacelle was 90 percent of the design value, at an air-flow rate of 74 percent of design. These figures are subject to a slight correction for air flow to the inboard section.

CONCLUSIONS

1. Present available data on heat flow are adequate to permit the design of thermal ice-prevention equipment for metal airplanes on the basis of required temperature rise at specified locations. Preliminary flight tests of the B-17F installation, under non-icing conditions, indicate that the design temperatures are, with minor exceptions, realized.

2. Based upon experience gained in flights under natural icing conditions with previous similar designs, the heat flow in the system described for the B-17F airplane is sufficient to provide satisfactory ice protection for the wing outer panels, but may be inadequate for the empennage and wing tips.

Ames Aeronautical Laboratory,
National Advisory Committee for Aeronautics,
Moffett Field, Calif.

REFERENCES

1. Rodert, Lewis A., Clousing, Lawrence A., and McAvoy, William H.: Recent Flight Research on Ice Prevention. A.R.R., NACA, Jan. 1942.
2. Jones, Alun R., and Rodert, Lewis A.: Development of Thermal Ice-Prevention Equipment for the B-24D Airplane. A.C.R., NACA, Feb. 1943.

TABLE I - ENGINE DATA RECORDED DURING FLIGHT TESTS
OF B-17F THERMAL ICE-PREVENTION EQUIPMENT

Flight	1	2
Pressure altitude, feet	10,000	18,000
Free air temperature, °F	40	44
Correct indicated air speed, mph	155	155
Manifold pressure, inches of mercury:		
Engine 1	26.3	-----
Engine 3	26.5	26.0
Engine 4	26.5	25.7
Revolutions per minute:		
Engine 1	1,980	-----
Engine 3	2,030	2,000
Engine 4	2,000	2,000

TABLE II. - RESULTS OF FLIGHT TESTS OF THERMAL
ICE-PREVENTION EQUIPMENT IN RIGHT WING OUTER PANEL, B-17F AIRPLANE

Thermo- couple	Flight	1	2
	Pressure altitude, feet	10,000	18,000
	Correct indicated airspeed, mph	155	155
G1	Temperature of gas into exchanger 4, °F	1,640	-----
G2	Temperature of gas out of exchanger 4, °F	1,510	-----
	Free air temperature, °F	40	-4
	² Weight of air to outboard section, pounds per hour	2,290	1,940
A40	Temperature of air into exchanger 4, °F	40	-4
A41	Temperature of air out of exchanger 4, °F	352	390
	Temperature rise, °F	312	394
	Heat to air, Btu per hour	171,500	184,000
	Air temperatures, °F		
A7	Air into gap, station 20	251	262
A8	Air at upper gap exit, station 20	82	65
A9	Air at lower gap exit, station 20	98	70
A14	Air in wing near aileron gap, station 20	62	40
A11	Air into gap, station 22 $\frac{1}{2}$	338	351
A4	Air into gap, station 25	308	341
A5	Air at upper gap exit, station 25	106	103
A6	Air at lower gap exit, station 25	155	140
A13	Air in wing near aileron gap, station 24 $\frac{1}{2}$	68	45

¹Numbers correspond to thermocouple locations on fig. 33.

²Measured at 5-in. venturi.

TABLE II (Continued)

Thermo- couple	Flight	1	2
A10	Air into gap, station 29	308	321
A1	Air into gap, station 33	267	287
A2	Air at upper gap exit, station 33	137	122
A3	Air at lower gap exit, station 33	152	145
A12	Air in wing near aileron gap, station 32	94	84
A28	Air into gap, wing tip, station 35	132	112
Skin temperatures, °F above free air temperature			
S76	Intercooler air intake lip at 5-percent chord, station 15 $\frac{1}{2}$	40	59
S75	Carburetor air intake lip at 5-percent chord, station 16 $\frac{1}{2}$	40	59
S25	On nose, station 20	130	145
S26	Upper at 3-percent chord, station 20	94	116
S27	Lower at 3-percent chord, station 20	105	126
S28	Upper at 8-percent chord, station 20	45	59
S29	Lower at 8-percent chord, station 20	76	98
S30	Upper at 13-percent chord, station 20	30	44
S31	Lower at 13-percent chord, station 20	50	59
S39	Upper near aileron gap, station 20	14	29
S20	On nose, station 22 $\frac{1}{2}$	217	271
S21	Upper at 3-percent chord, 22 $\frac{1}{2}$	160	197
S22	Lower at 3-percent chord, station 22 $\frac{1}{2}$	180	229
S23	Upper at 12-percent chord, station 22 $\frac{1}{2}$	68	93

TABLE II (Continued)

Thermo- couple	Flight	1	2
S24	Lower at 12-percent chord, station $22\frac{1}{2}$	125	149
S13	On nose, station 25	183	229
S14	Upper at 4-percent chord, station 25	150	186
S15	Lower at 4-percent chord, station 25	180	224
S16	Upper at 8-percent chord, station 25	70	98
S17	Lower at 8-percent chord, station 25	130	159
S18	Upper at 13-percent chord, station 25	51	74
S19	Lower at 13-percent chord, station 25	112	135
S52	Upper at 25-percent chord, station $24\frac{1}{2}$	30	54
S53	Lower at 25-percent chord, station $24\frac{1}{2}$	25	44
S33	Upper at 35-percent chord, station $24\frac{1}{2}$	27	49
S34	Lower at 35-percent chord, station $24\frac{1}{2}$	15	29
S54	Upper at 50-percent chord, station $24\frac{1}{2}$	25	44
S55	Lower at 50-percent chord, station $24\frac{1}{2}$	17	29
S35	Upper at 65-percent chord, station $24\frac{1}{2}$	18	39
S36	Lower at 65-percent chord, station $24\frac{1}{2}$	15	24
S37	Upper near aileron gap, station $24\frac{1}{2}$	20	44
S38	Lower near aileron gap, station $24\frac{1}{2}$	17	29
S8	On nose, station 29	157	196
S9	Upper at 3-percent chord, station 29	135	164
S10	Lower at 3-percent chord, station 29	162	207
S11	Upper at 10-percent chord, station 29	68	98

TABLE II (Continued)

Thermo- couple	Flight	1	2
S12	Lower at 10-percent chord, station 29	123	149
S1	On nose, station 33	127	154
S2	Upper at 3-percent chord, station 33	160	202
S3	Lower at 3-percent chord, station 33	112	145
S4	Upper at 8-percent chord, station 33	35	103
S5	Lower at 8-percent chord, station 33	127	154
S6	Upper at 11-percent chord, station 33	70	98
S7	Lower at 11-percent chord, station 33	105	135
S32	Upper at 65-percent chord, station 32	22	49
S56	On nose, wing tip, station 35	42	74
S57	Upper, wing tip at 5-percent chord, station 35	42	74
S58	Lower, wing tip at 5-percent chord, station 35	22	54
Structure temperatures, °F			
M3	On rib at 7-percent chord, station 20	122	103
M2	On rib at 7-percent chord, station 25	162	141
M1	On rib at 7-percent chord, station 33	150	126
Pressure orifice	Flight	1	2
Pressures in inches of water referred to cabin static pressure (+ above, - below)			
P _{S10}	Static at entrance to 5-inch venturi	-2.4	-3.7
P _{S11}	Static at throat of 5-inch venturi	+4.0	+3.2

TABLE III. - RESULTS OF FLIGHT TESTS OF THERMAL ICE-PREVENTION EQUIPMENT
IN RIGHT WING INNER PANEL AND EMPENNAGE, B-17F AIRPLANE

Thermo- couple	Flight	1	2
	Pressure altitude, feet	10,000	18,000
	Correct indicated airspeed, mph	155	155
	Free air temperature, °F	+32	-4
A42	Temperature of air out of exchanger 3, °F	353	395
	Temperature rise, °F	321	399
	Weight of air to empennage, pounds per hour	2,450	1,960
	¹ Heat capacity, exchanger 3, Btu per hour	189,000	186,000
	Wing inner panel, air temperatures, °F		
A39	In duct at 8-percent chord, station 9	285	316
A38	At gap exit at 8-percent chord, station 9	77	50
	Wing inner panel, skin temperatures, °F above free air temperature		
S74	Lower at 7-percent chord, station 9	128	164
S72	Lower at 4-percent chord, station 9	90	121
S70	On nose, station 9	65	88
S71	Upper at 4-percent chord, station 9	32	44
S73	Upper at 7-percent chord, station 9	17	29
	Wing inner panel, structure temperatures, °F		
M11	On rib at 4-percent chord, station 9	93	60

¹Neglecting small amount of air flow to wing inner panel.

TABLE III (Continued)

Thermo- couple	Flight	1	2
	Right stabilizer air temperatures, °F		
A35	Air into gap, inboard station	117	103
A36	At upper gap exit, inboard station	55	20
A37	At lower gap exit, inboard station	65	35
A32	Air into gap, center station	141	131
A33	At upper gap exit, center station	99	80
A34	At lower gap exit, center station	108	84
A29	Air into gap, outboard station	117	103
A30	Air at upper gap exit, outboard station	84	50
A31	Air at lower gap exit, outboard station	80	40
	Right stabilizer skin temperatures, °F above free air temperature		
S67	On nose, inboard station	28	34
S68	Upper near air exit, inboard station	23	29
S69	Lower near air exit, inboard station	28	24
S62	On nose, center station	76	88
S63	Upper near air exit, center station	57	64
S64	Lower near air exit, center station	52	64
S65	Upper at 20-percent chord, center station	23	24
S66	Lower at 20-percent chord, center station	18	24
S59	On nose, outboard station	76	88
S60	Upper near air exit, outboard station	52	44
S61	Lower near air exit, outboard station	52	44

TABLE III (Continued)

Thermo- couple	Flight	1	2
	Right stabilizer structure temperature, °F		
M10	On rib, inboard station	94	65
M9	On rib, center station	141	126
M8	On spar baffle, outboard station	80	45
	Dorsal air temperatures, °F		
A24	Air into gap, bottom station	306	341
A25	Air into gap, top station	214	225
A26	Air at left gap exit, top station	80	50
A27	Air at right gap exit, top station	84	55
	Dorsal skin temperatures, °F above free air temperature		
S49	On nose, top station	76	98
S50	Left skin near air exit, top station	71	88
S51	Right skin near air exit, top station	62	74
	Dorsal structure temperature, °F		
M7	On rib, top station	160	155
	Fin air temperatures, °F		
A15	Air into gap, bottom station	292	306
A16	At left gap exit, bottom station	---	---
A17	At right gap exit, bottom station	160	122
A18	Air into gap, center station	171	166
A19	At left gap exit, center station	117	103

TABLE III (Concluded)

Thermo- couple	Flight	1	2
A20	At right gap exit, center station	94	60
A21	Air into gap, top station	94	60
A22	At left gap exit, top station	60	30
A23	At right gap exit, top station	70	40
Fin skin temperatures, °F above free air temperature			
S40	On nose, bottom station	128	144
S41	Left skin near air exit, bottom station	67	93
S42	Right skin near air exit, bottom station	80	84
S43	On nose, center station	85	107
S44	Left skin near air exit, center station	71	74
S45	Right skin near air exit, center station	71	84
S46	On nose, top station	33	39
S47	Left skin near air exit, top station	28	29
S48	Right skin near air exit, top station	33	29
Fin structure temperatures, °F			
M4	On spar baffle, bottom station	94	70
M5	On spar baffle, center station	131	117
M6	On spar baffle, top station	70	45
Pressure orifice	Flight	1	2
Pressures in inches of water referred to cabin static pressure (+ above, - below)			
P _{S12}	6-inch venturi throat static in empennage supply duct	+1.90	+2.05
P _{S13}	6-inch venturi lip static in empennage supply duct	+5.69	+5.50

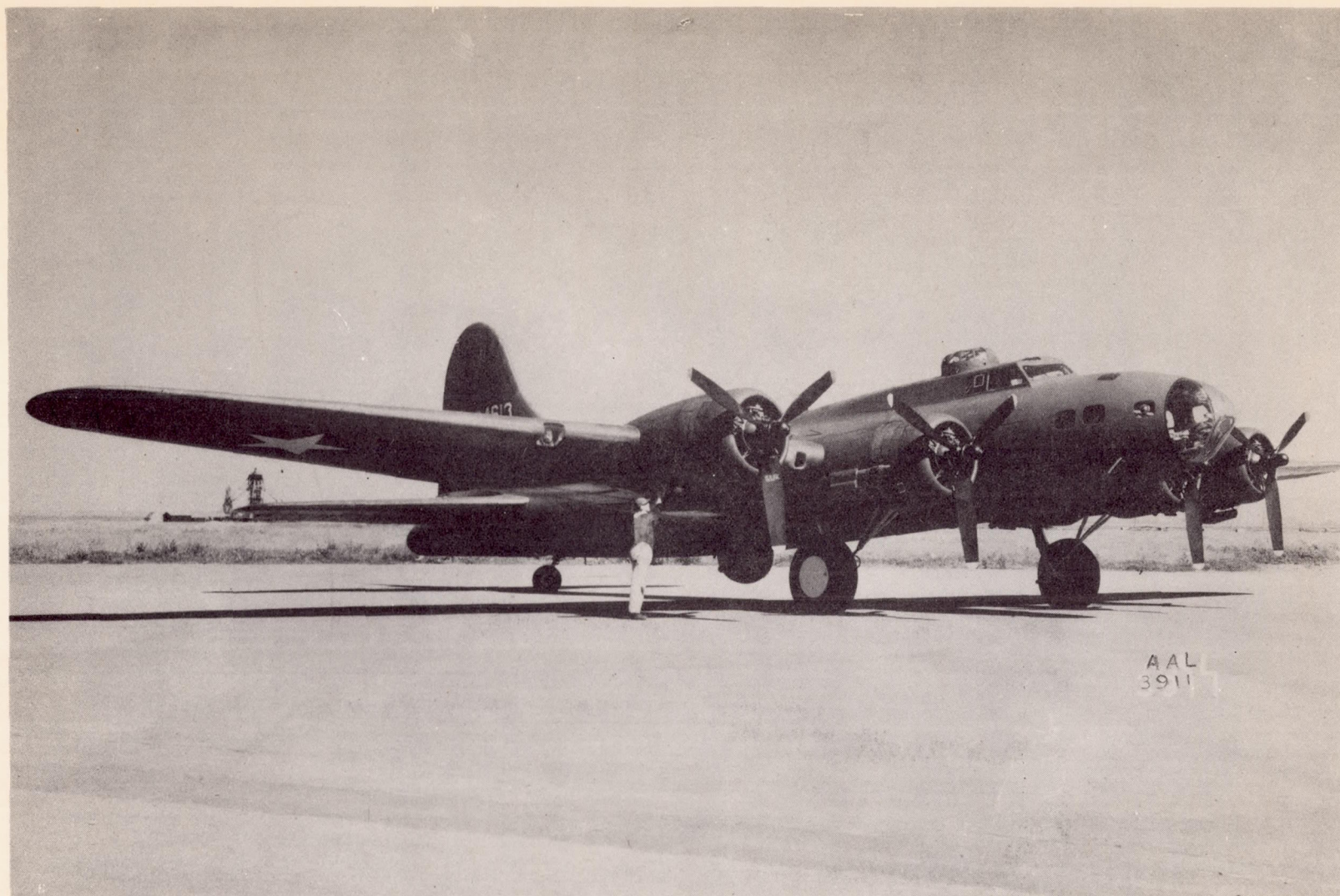


Figure 1.- The B-17F airplane in which thermal ice-prevention equipment was installed and tested.

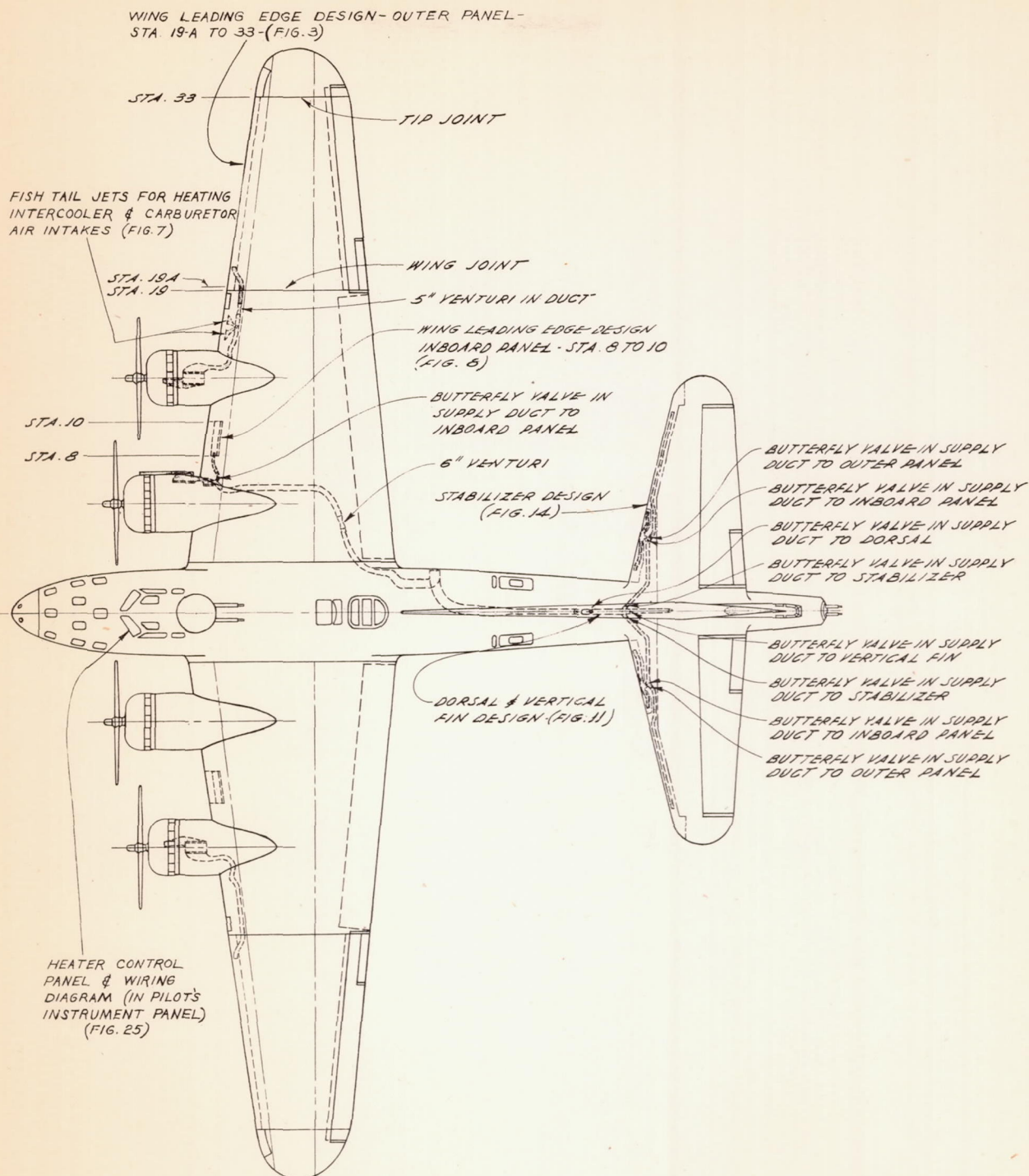


Figure 2.- General view of thermal ice-prevention system, B17F airplane.

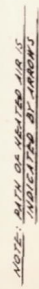


Figure 3.- Details of wing outer-panel leading-edge design for B-17F thermal ice-prevention system.

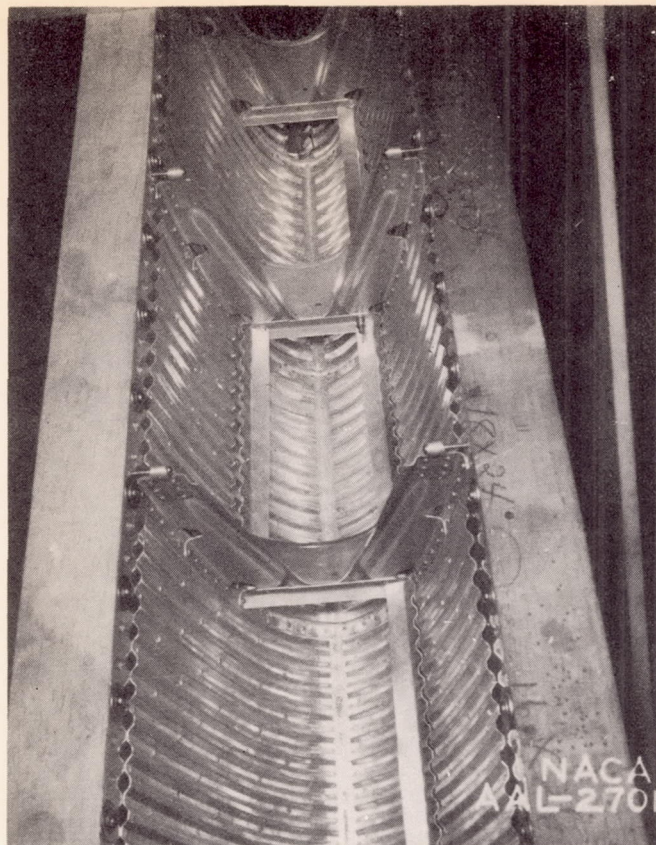


Figure 4.- Wing outer-panel leading-edge details for B-17F thermal ice-prevention system.

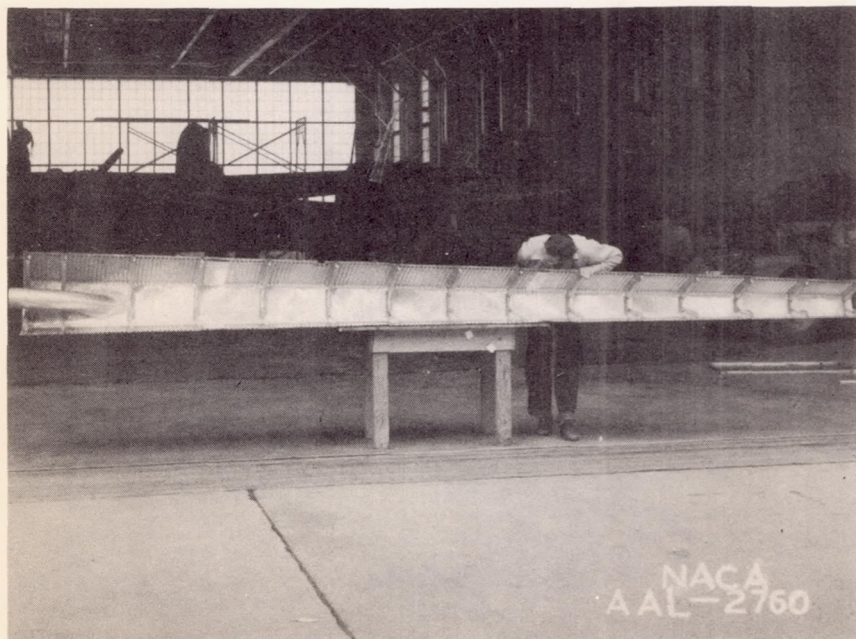
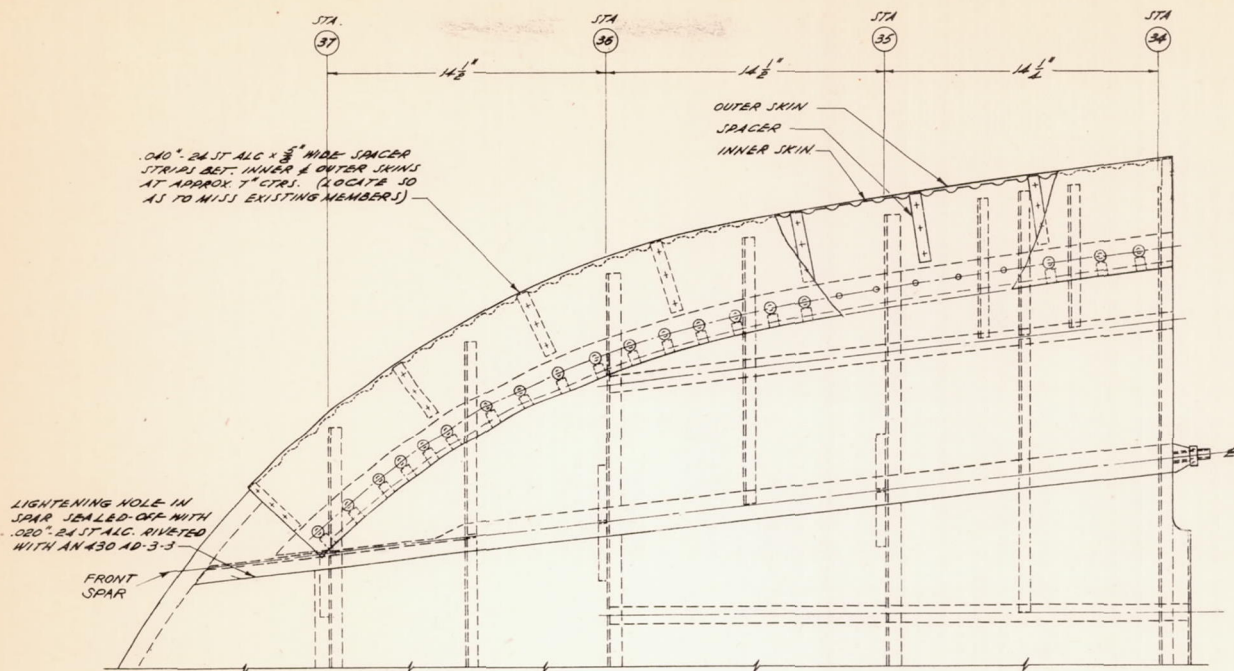


Figure 5.- Wing outer-panel leading-edge revised and ready for installation, B-17F airplane.



NOTE:
I.E. SPACER STRIPS ARE ATTACHED TO
INNER SKIN WITH BAC1341AD3-3
APPROX. 1 1/2" O.C.
B.A.C. STANDS FOR BOEING
AIRCRAFT COMPANY

LEFT WING TIP - LEADING EDGE (RIGHT WING OPP. HAND)

SCALE: 3" = 1'-0"

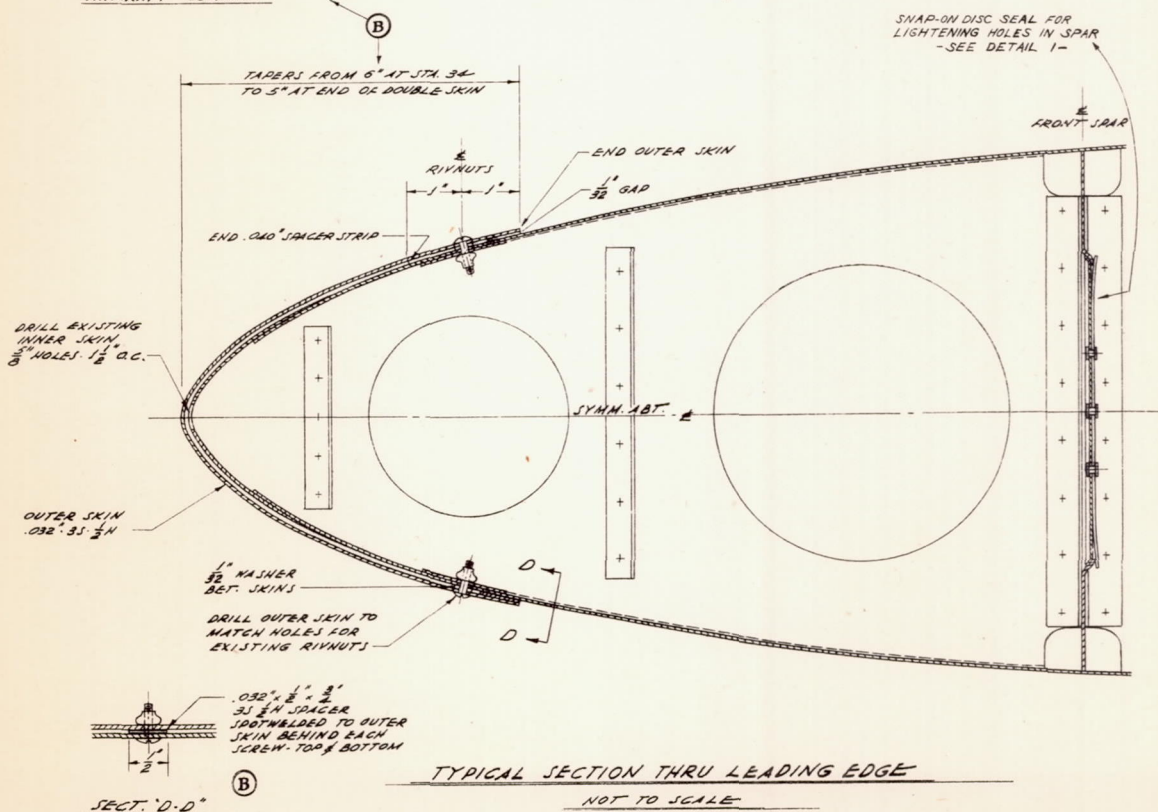


Figure 6.- Wing-tip details for B-17F thermal ice-prevention system.

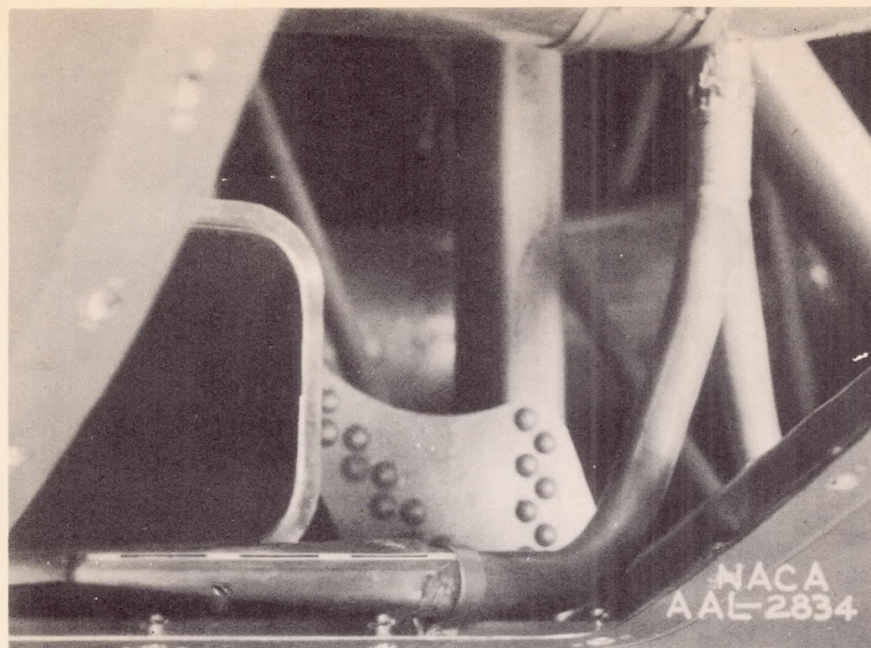


Figure 7.- Fish-tail type duct for heating lower edge of carburetor air intake for right outboard nacelle, B-17F airplane.

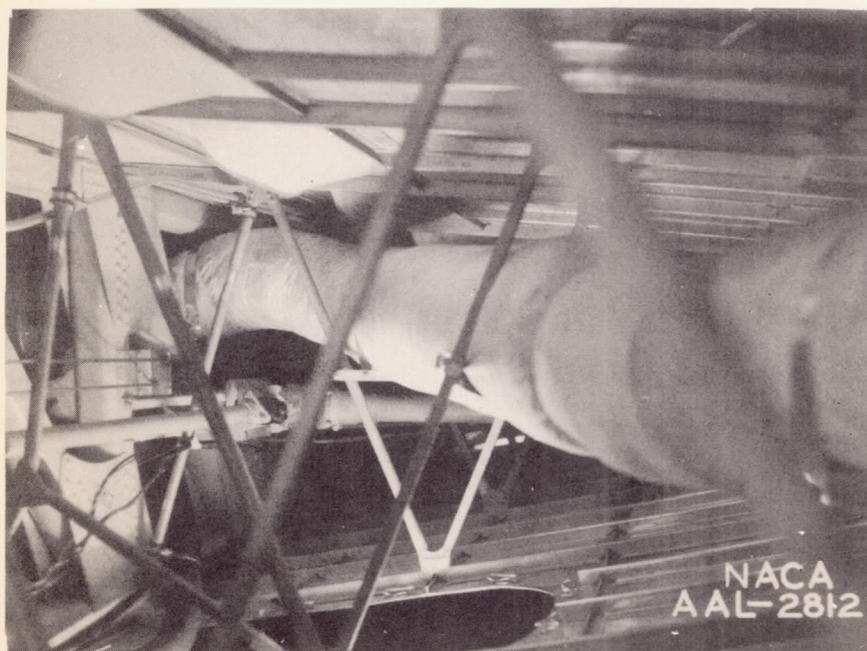


Figure 9.- View inside right wing of duct from inboard exchanger to fuselage, B-17F airplane.

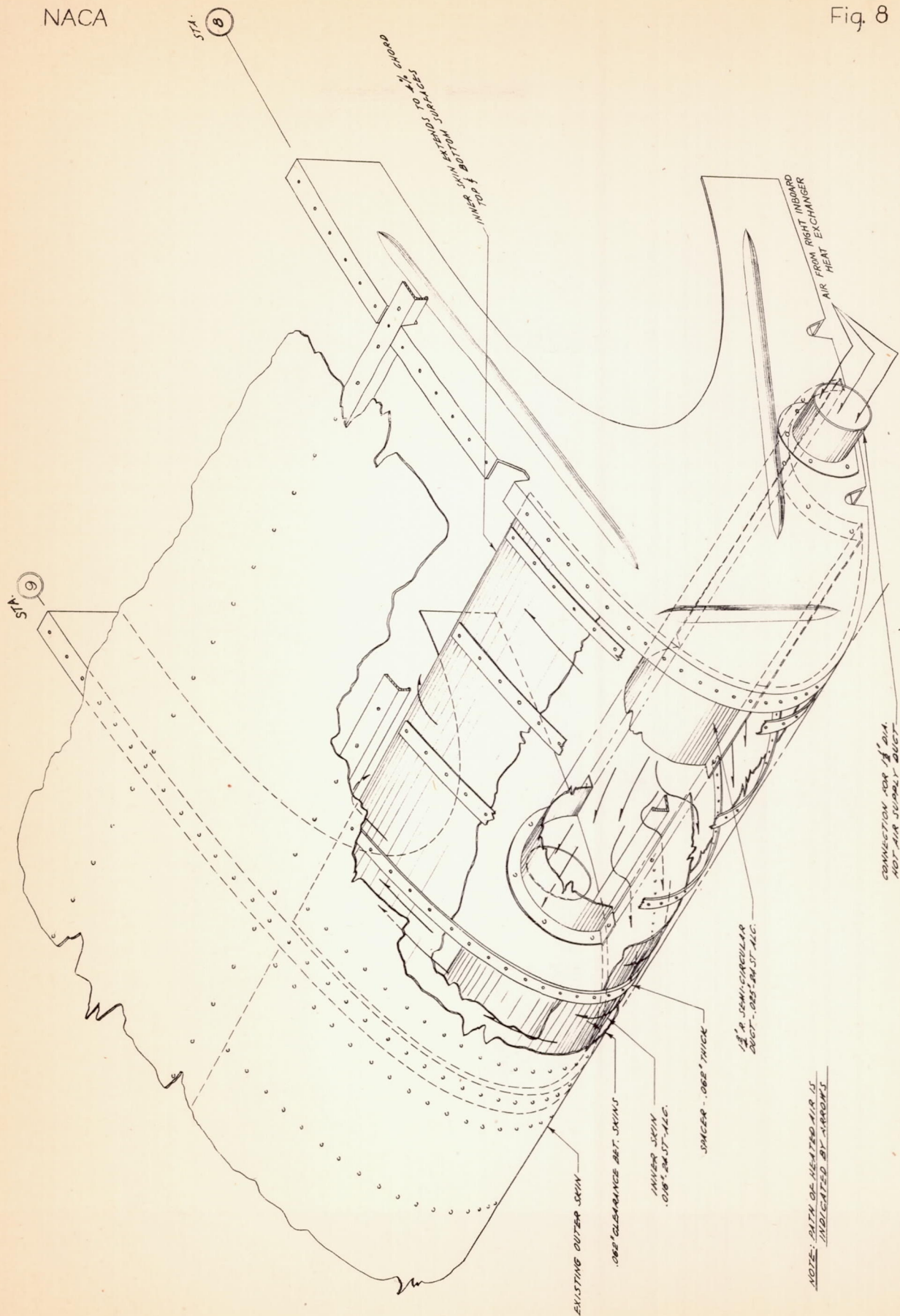


Figure 8.- Wing inboard panel leading-edge design (stations 8 to 10) for B-17F airplane thermal ice-prevention system.

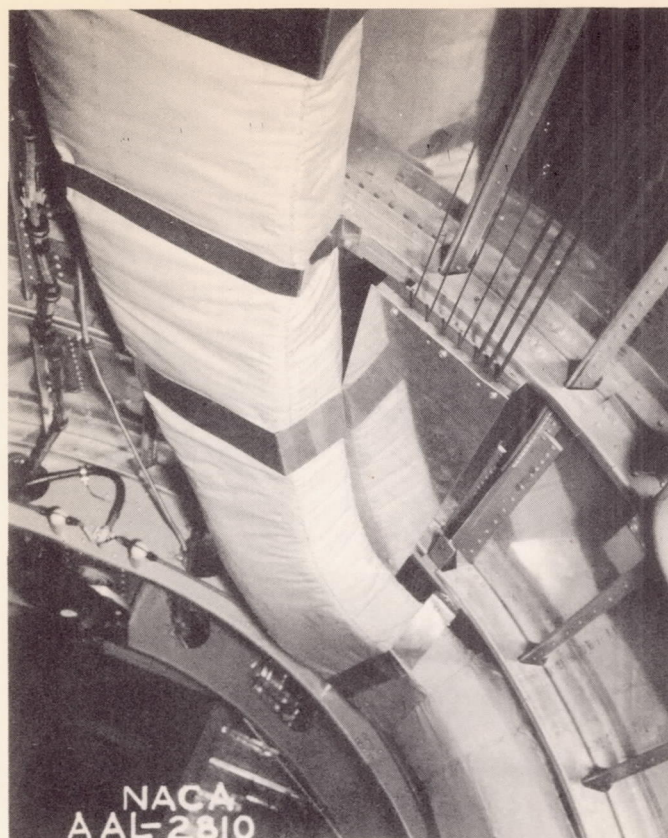


Figure 10.- View inside fuselage of empennage heated- air supply duct.

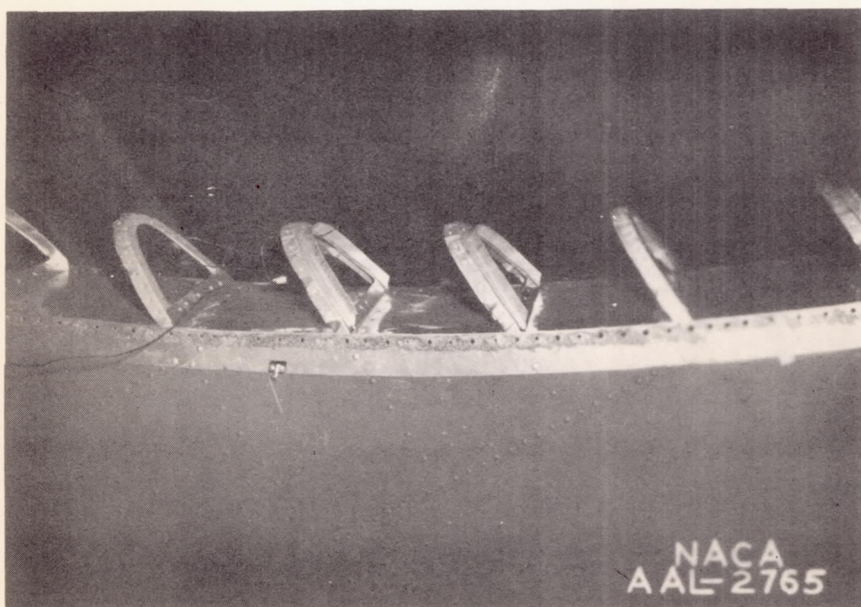


Figure 12.- Leading-edge rib alterations, typical for fin and dorsal, B-17F airplane.

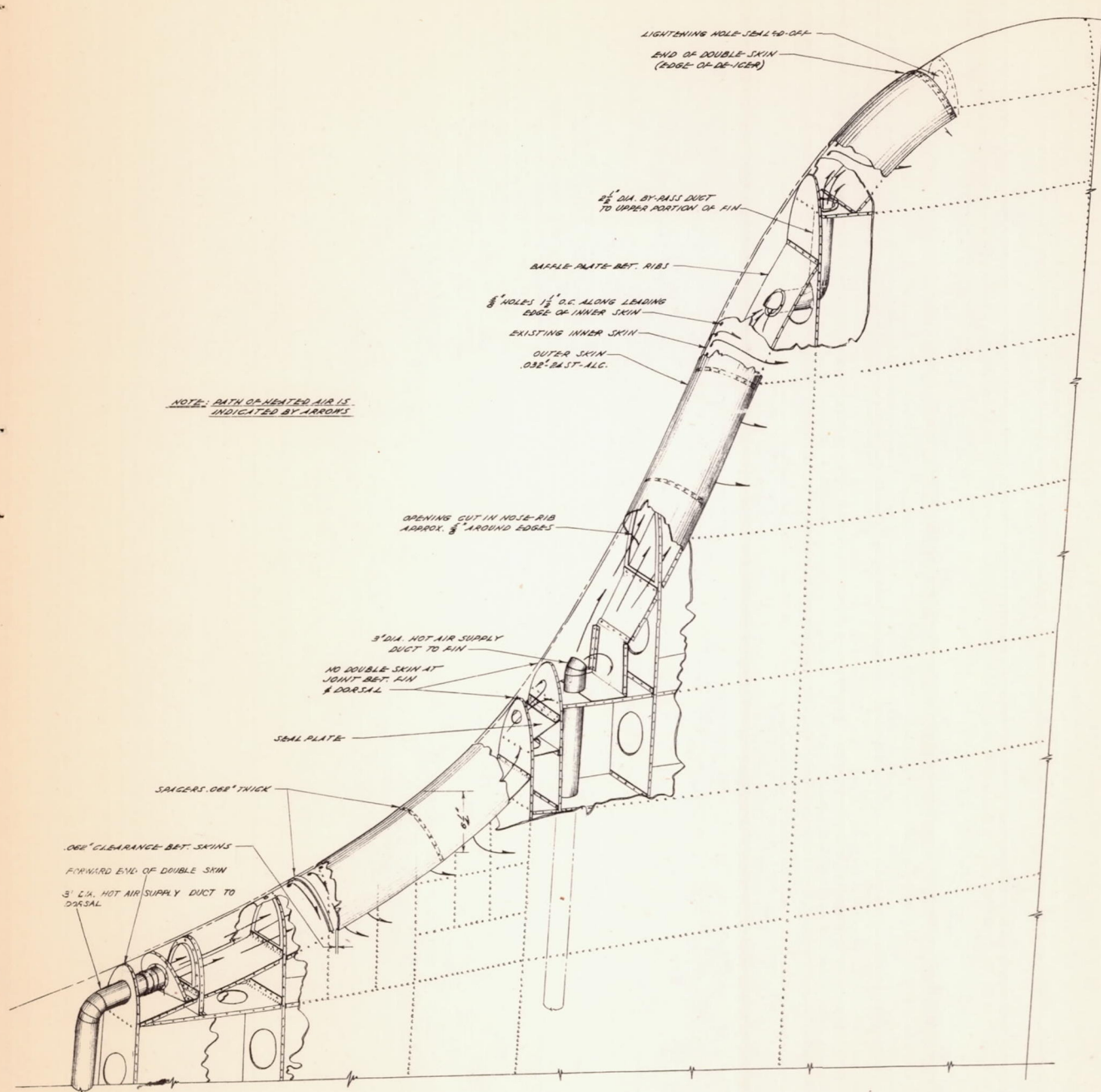


Figure 11.- Dorsal and fin design for B-17F thermal ice-prevention system.

A-51

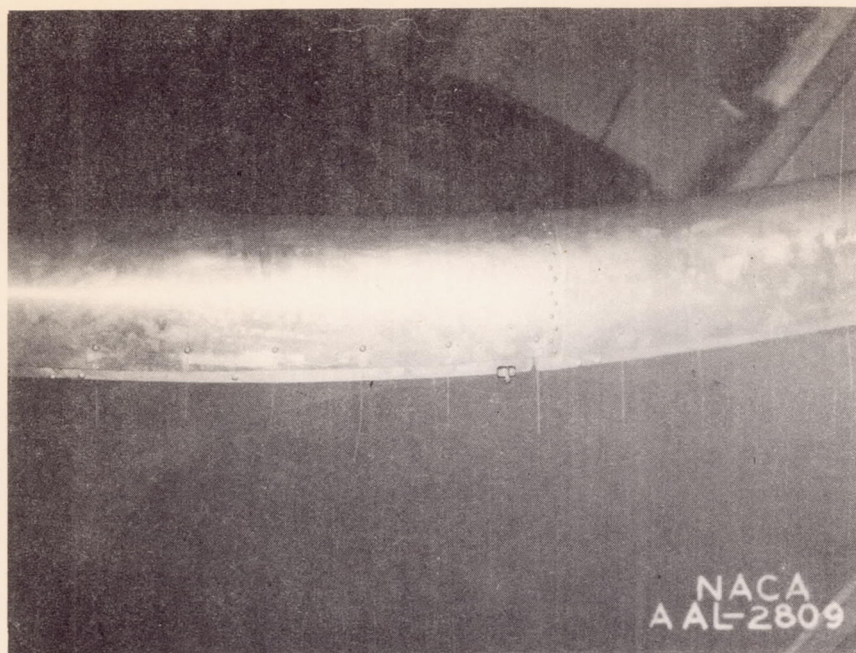


Figure 13.- Leading-edge outer skin installation, typical for fin and dorsal, B-17F airplane.

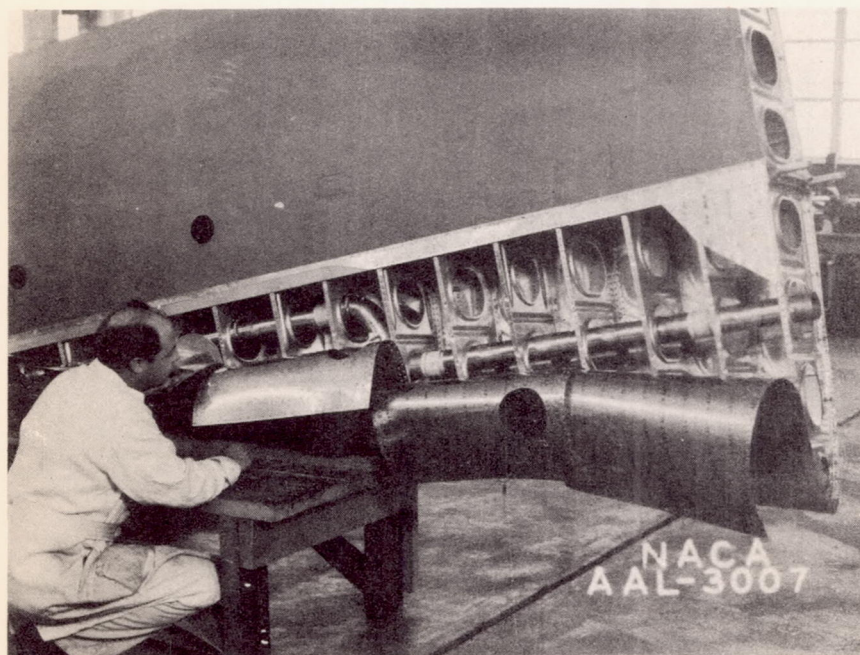


Figure 15.- Heated-air supply duct in inboard portion of horizontal stabilizer, B-17F airplane.

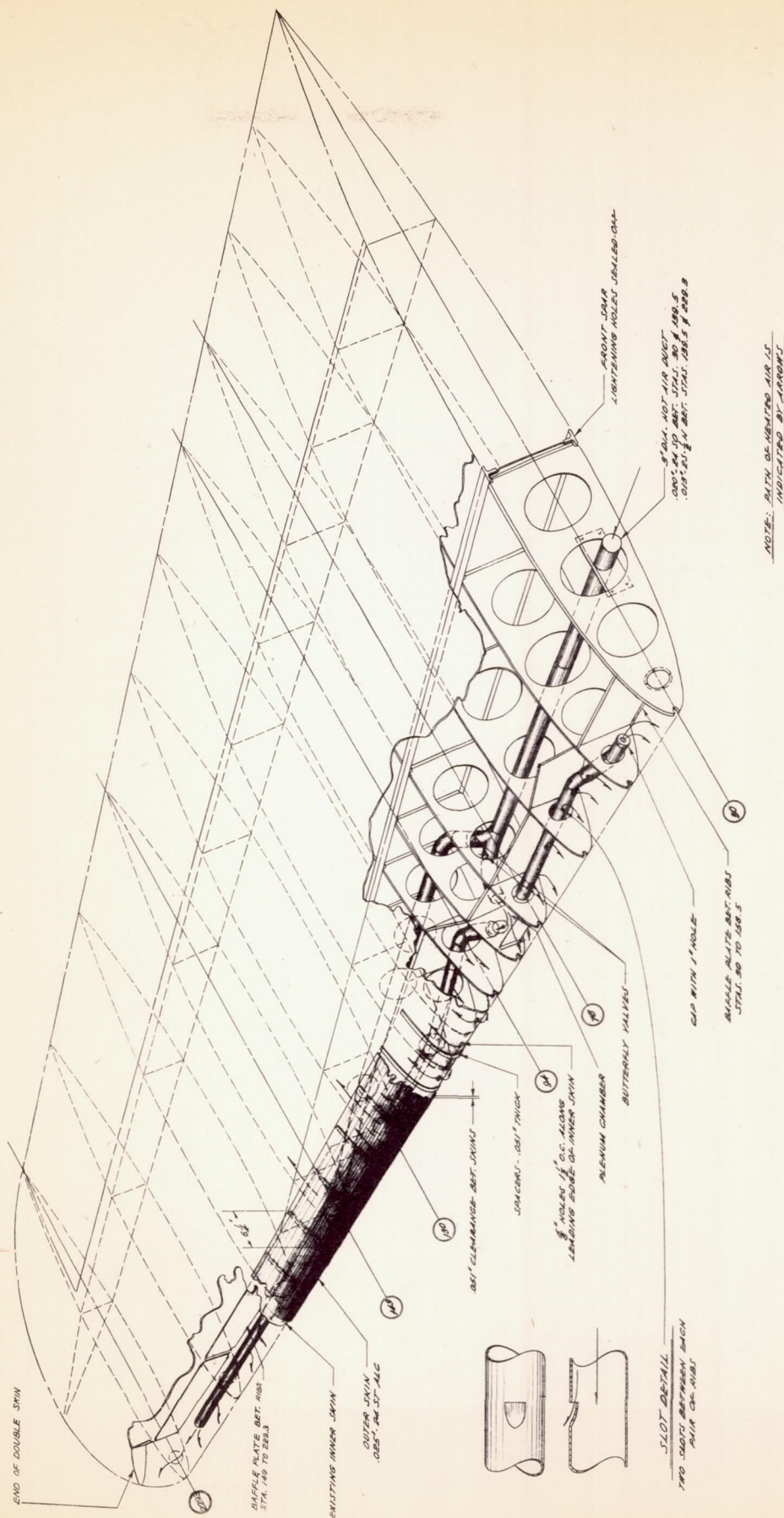


Figure 14- Stabilizer design for B-17F thermal ice-prevention system.

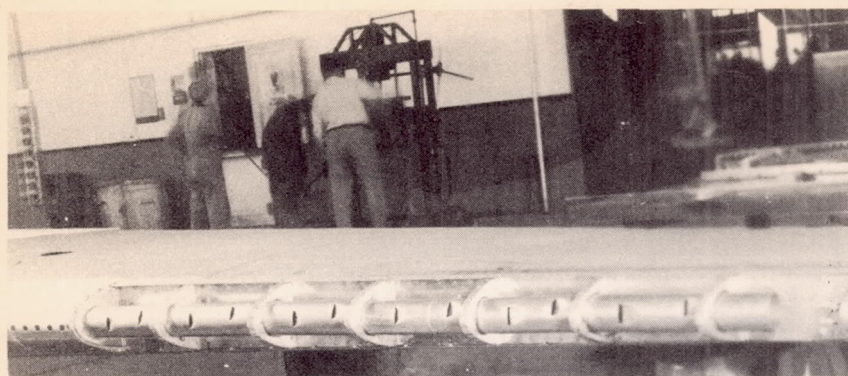


Figure 16.- Heated-air supply duct in leading-edge of outboard portion of B-17F horizontal stabilizer.

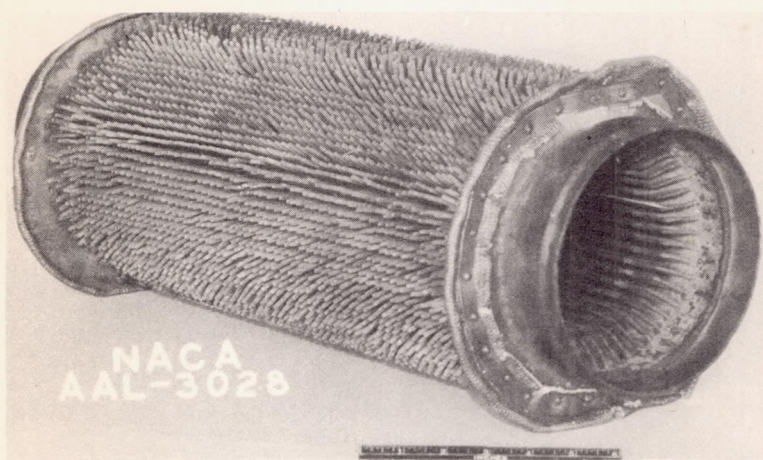


Figure 17.- Tail stack from outboard nacelle, B-17F airplane, as revised to provide more transfer surface for heat exchanger.

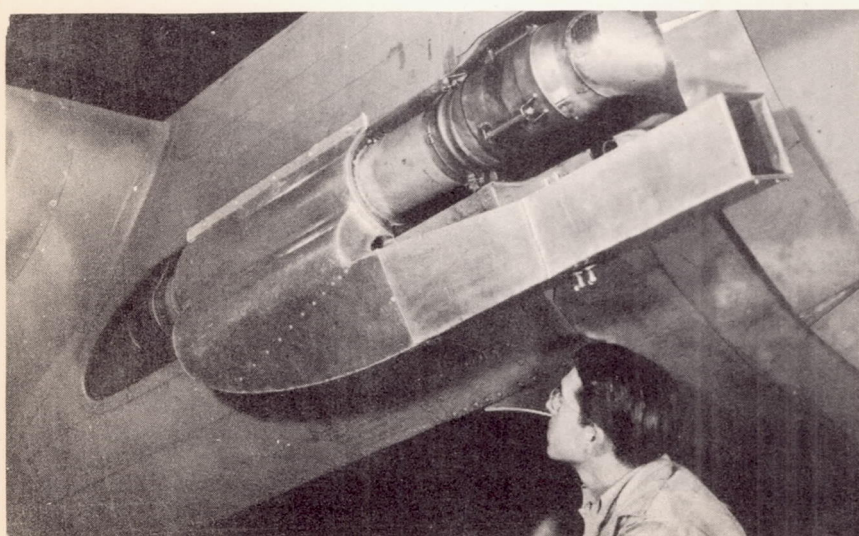


Figure 18.- Circulating air intake for heat exchanger in right inboard nacelle, B-17F airplane.

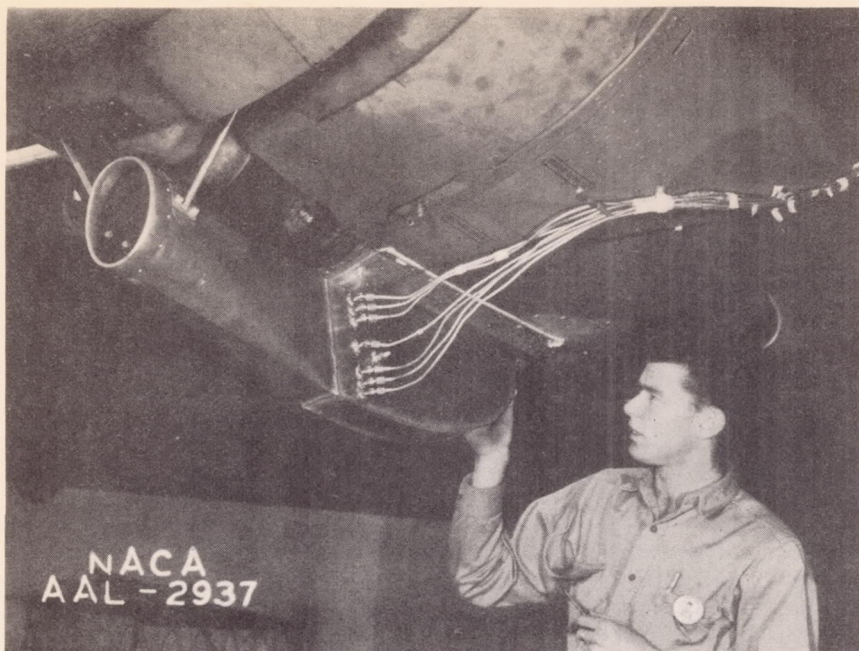


Figure 19.- Circulating air intake for heat exchanger in right outboard nacelle, B-17F airplane.

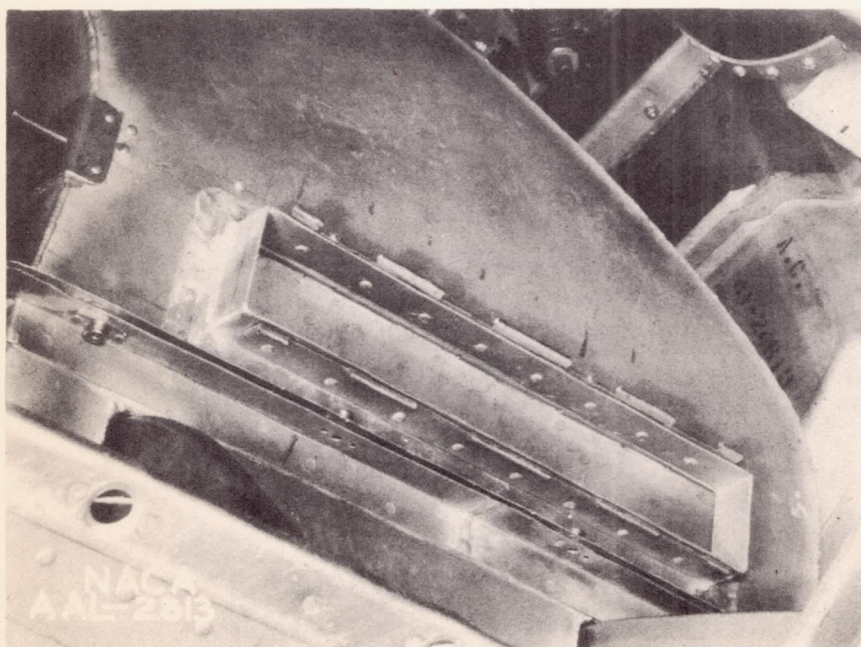


Figure 20.- Outlet for heated air from right outboard exchanger, B17F airplane.

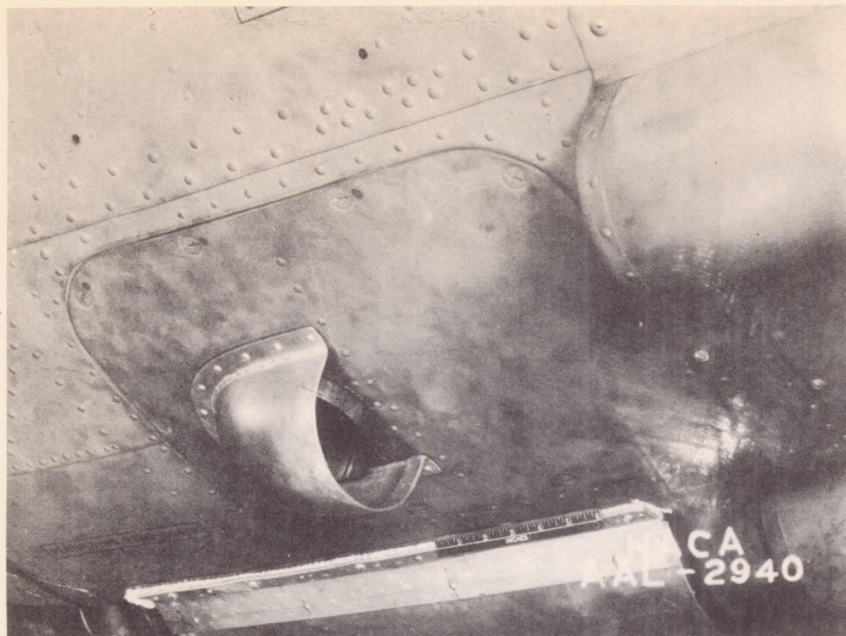


Figure 21.- Overboard dump for heated air from exchanger in left outboard nacelle, B-17F airplane.

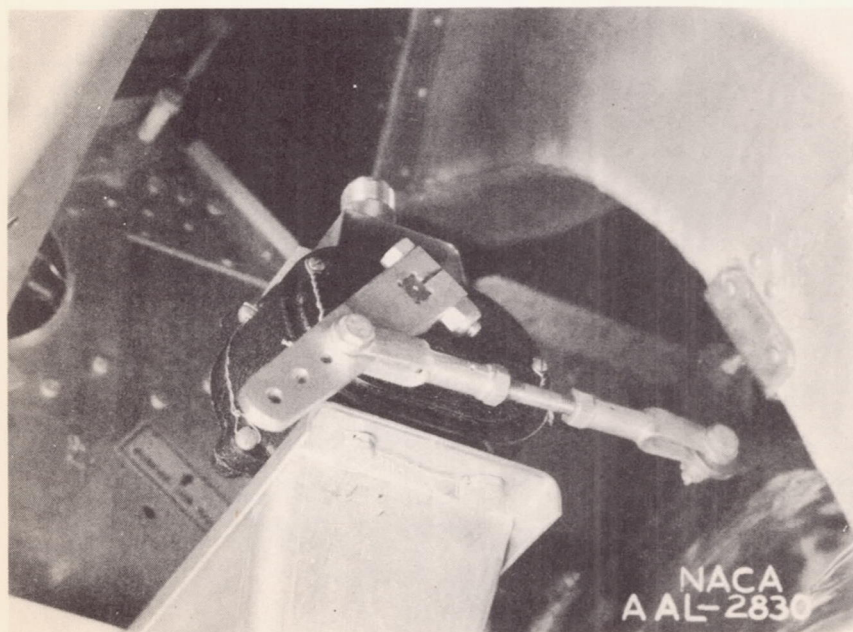


Figure 22.- Installation of dump-valve drive motor at exchanger outlet in right outboard nacelle, B-17F airplane.

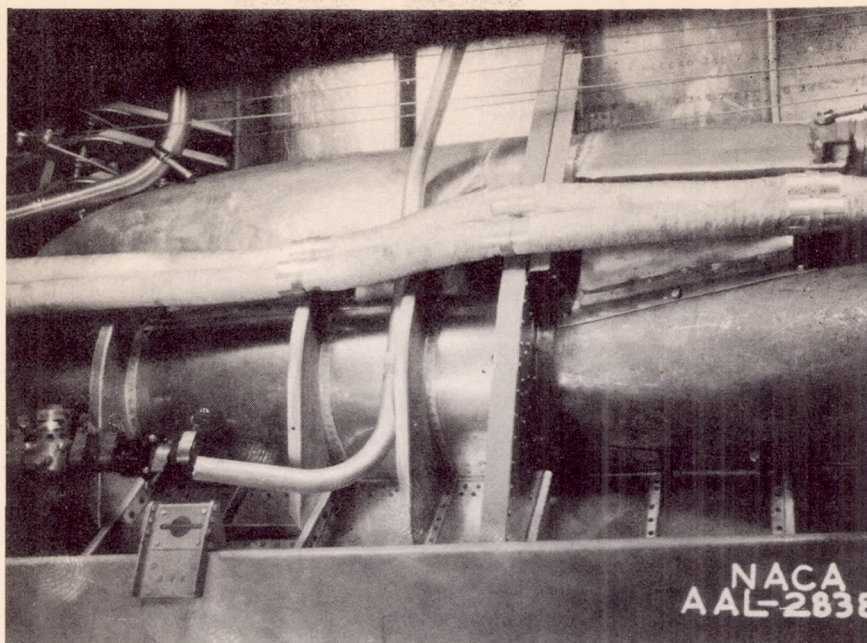


Figure 23.- Heated-air outlet and dump valve for exchanger installed in right inboard nacelle, B-17F airplane.

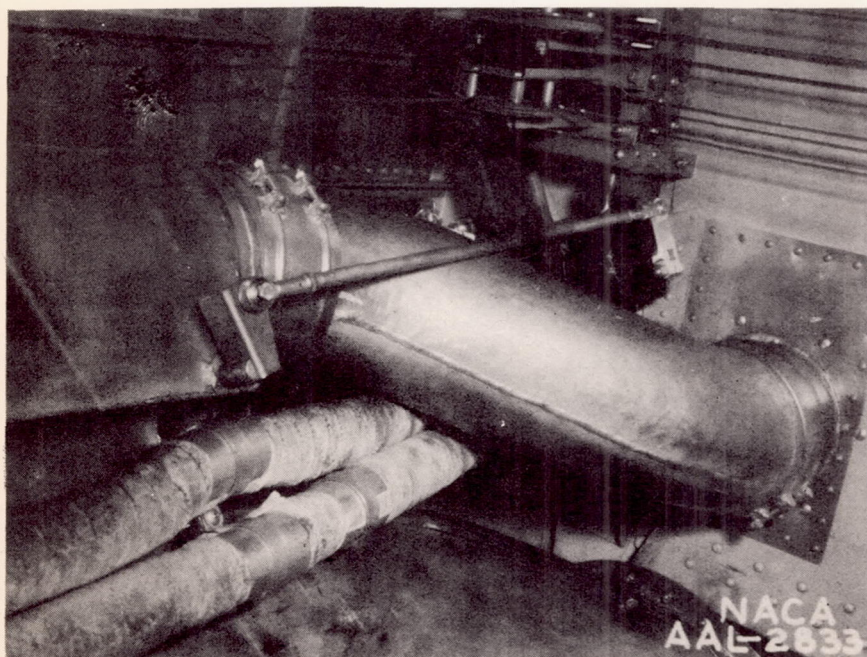


Figure 24.- Dump-valve and motor drive at outlet to exchanger in right inboard nacelle, B-17F airplane.

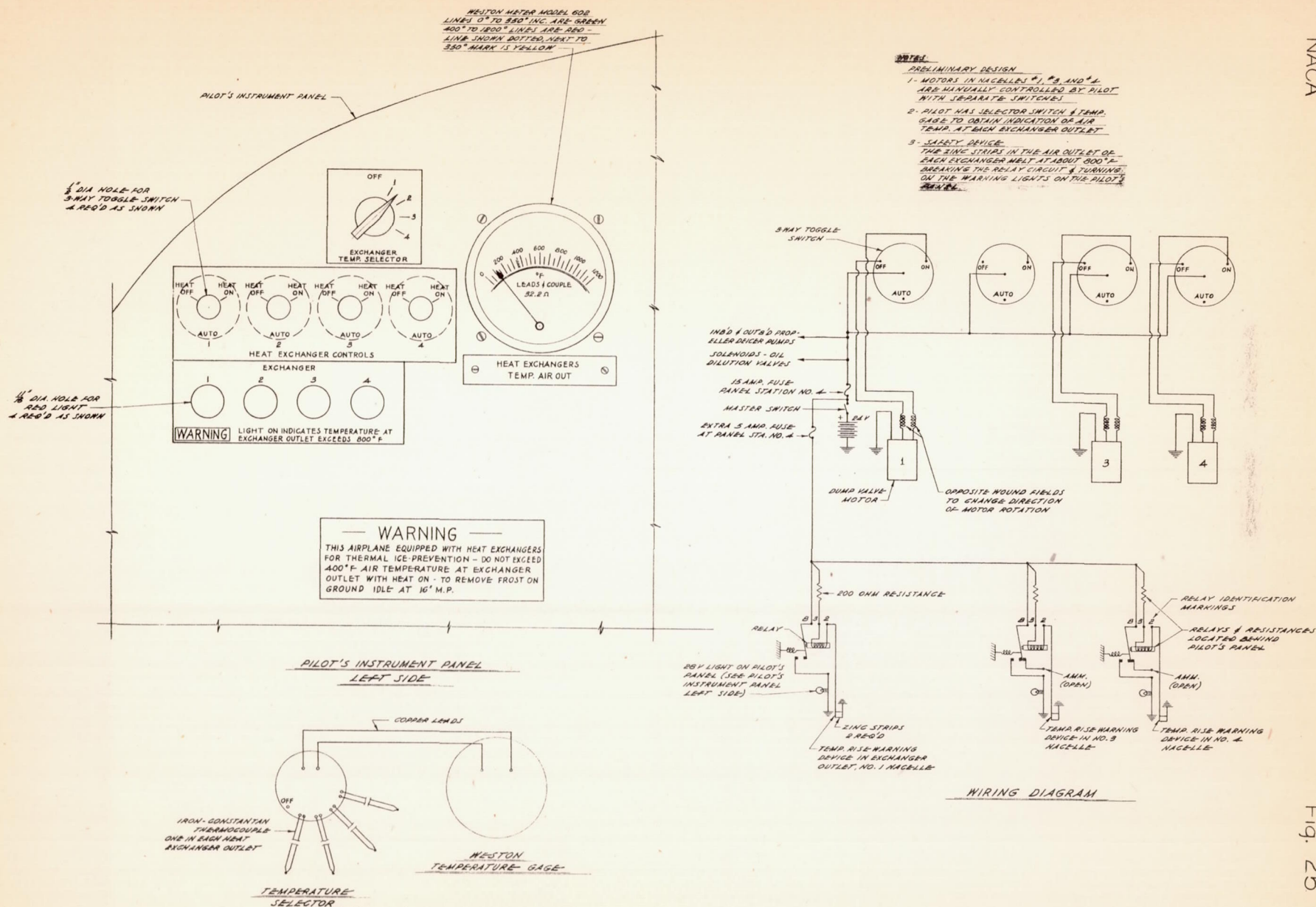


Figure 25.- Instrumentation and control for B-17F thermal ice-prevention system.

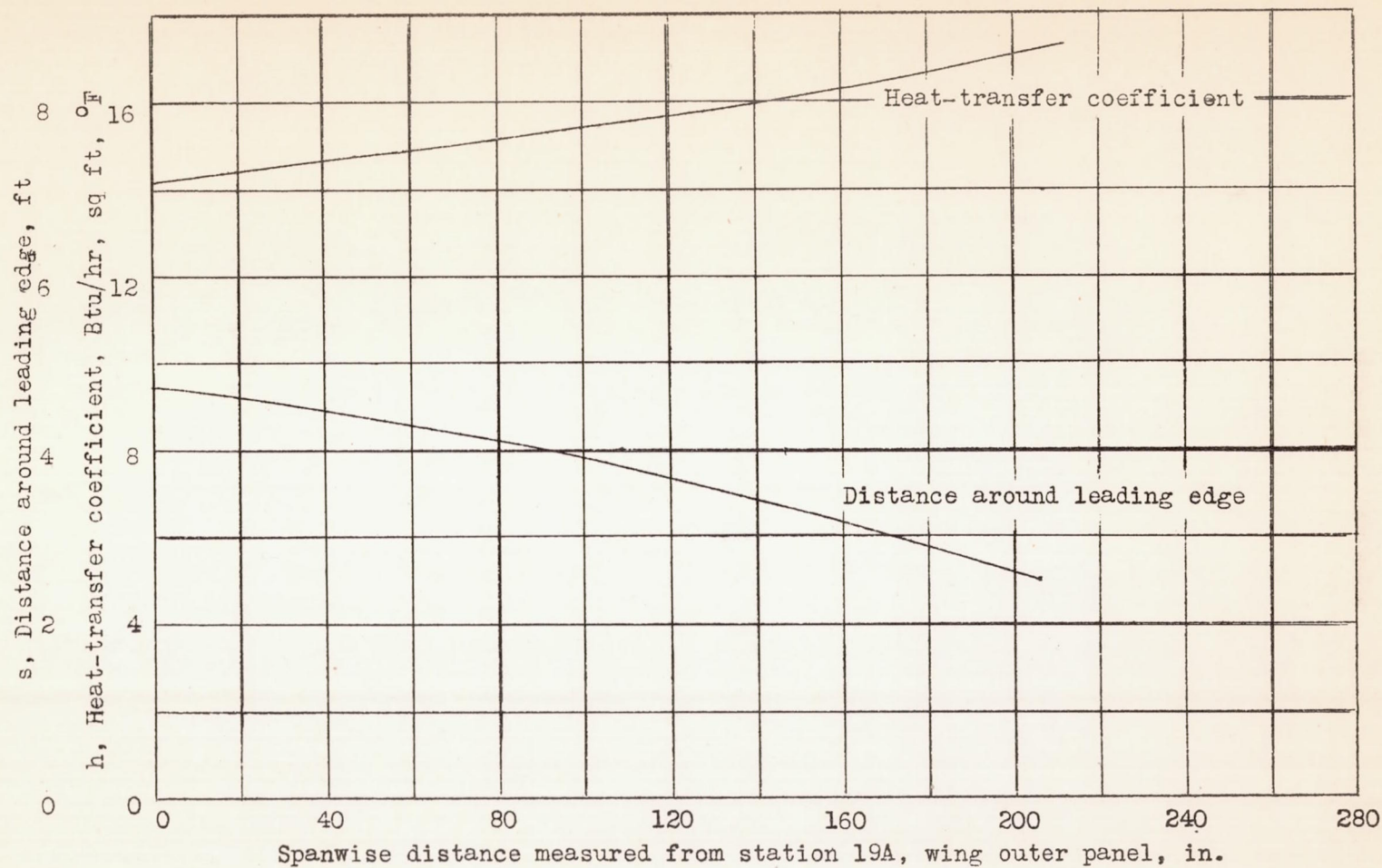
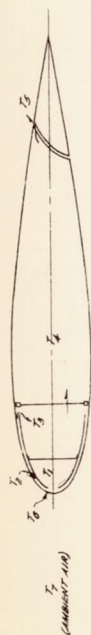


Figure 26.- Curves showing the distance around the leading edge from top to bottom of the front spar, and the heat-transfer coefficient for the leading edge of the wing outer panel, B-17F airplane.



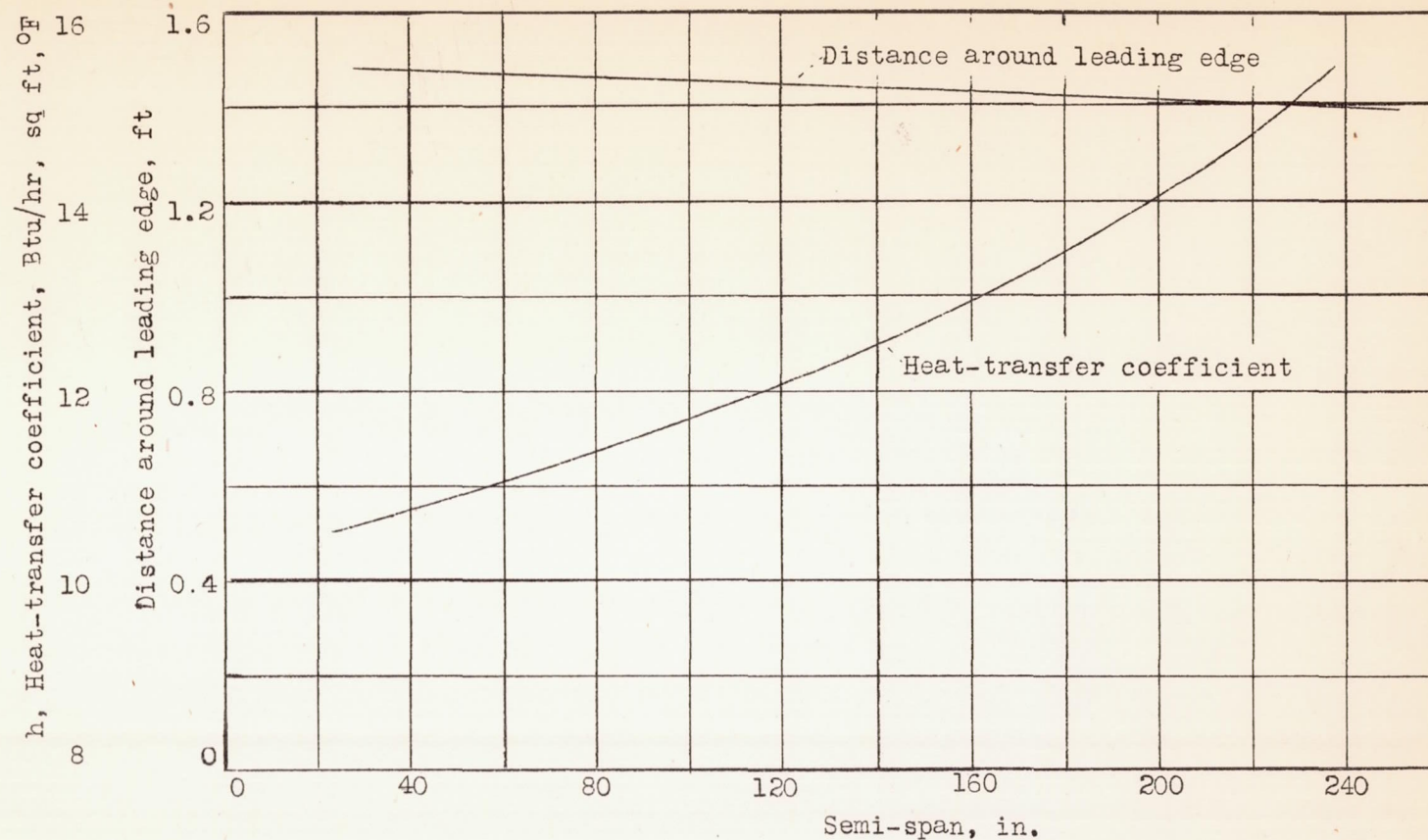


Figure 28.- Distance around the leading edge to be covered by double skin, and the heat-transfer coefficient for the leading edge of the horizontal stabilizer, B-17F airplane.

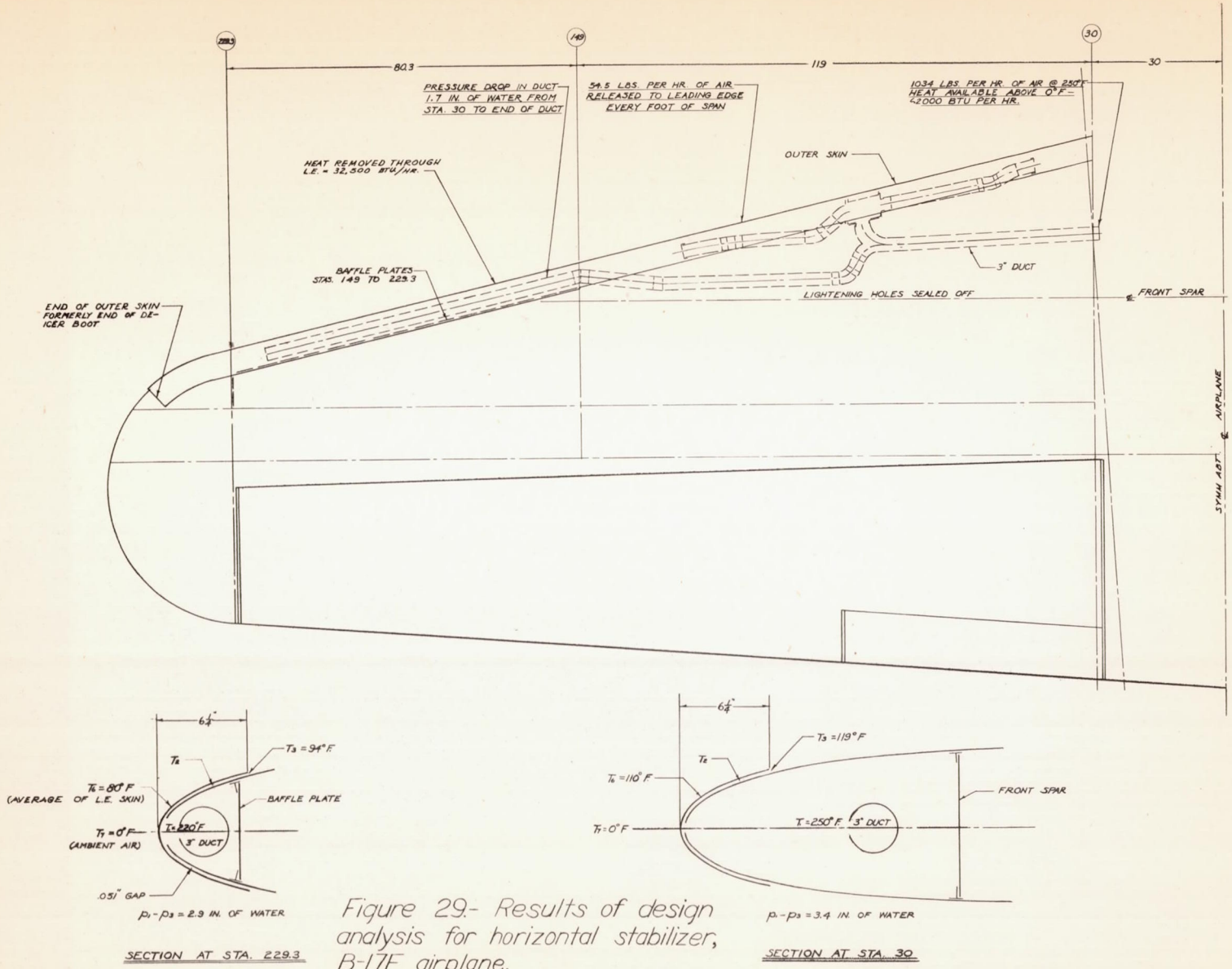


Figure 29.- Results of design analysis for horizontal stabilizer, B-17F airplane.

Fig. 29

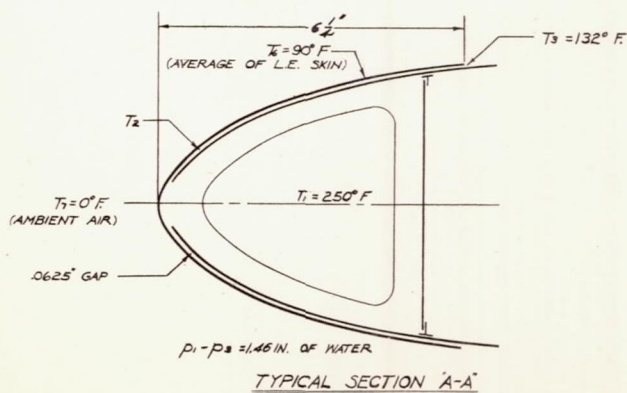
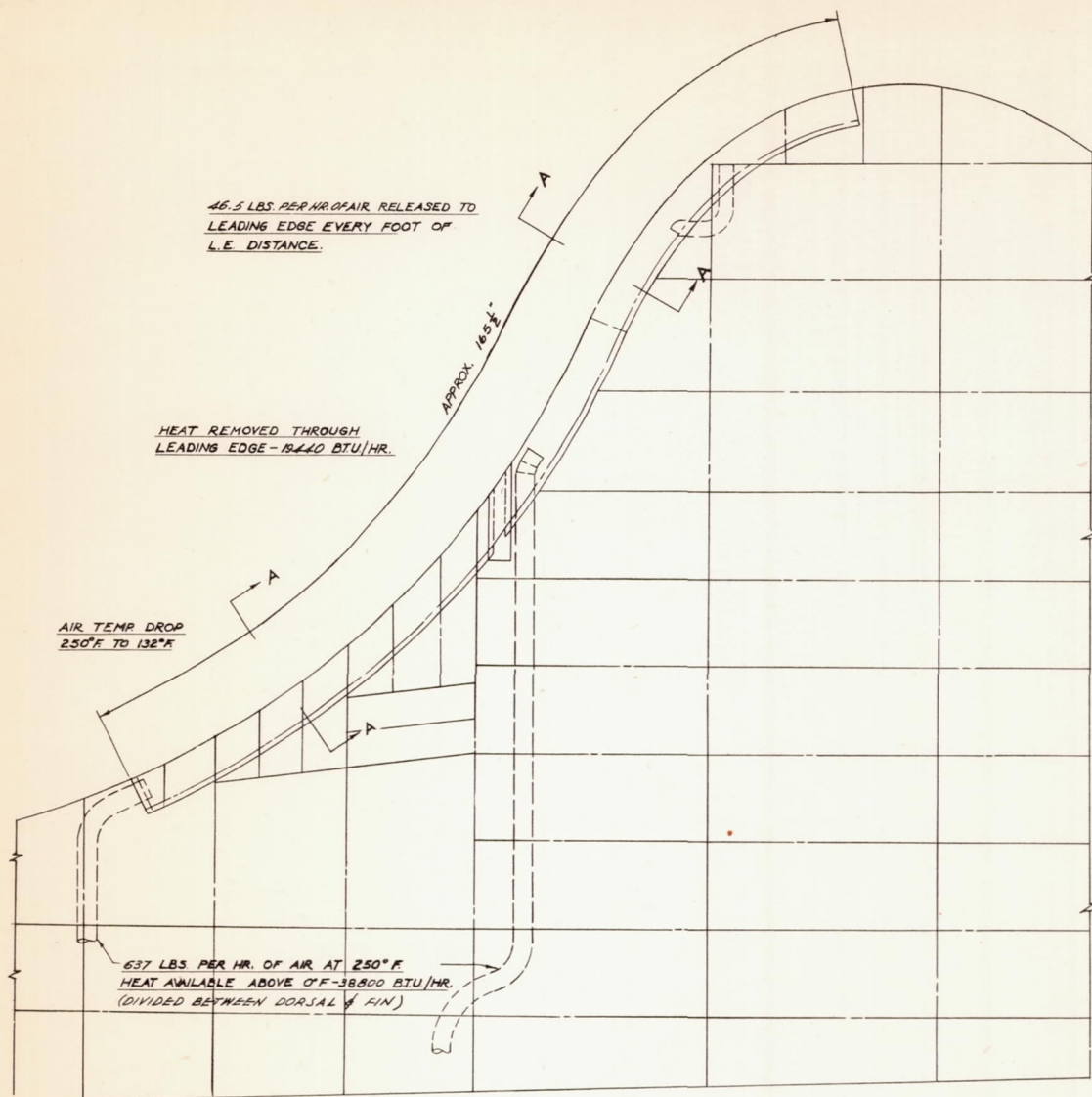


FIGURE 30- RESULTS OF DESIGN ANALYSIS FOR
FIN & DORSAL - B-17F AIRPLANE-

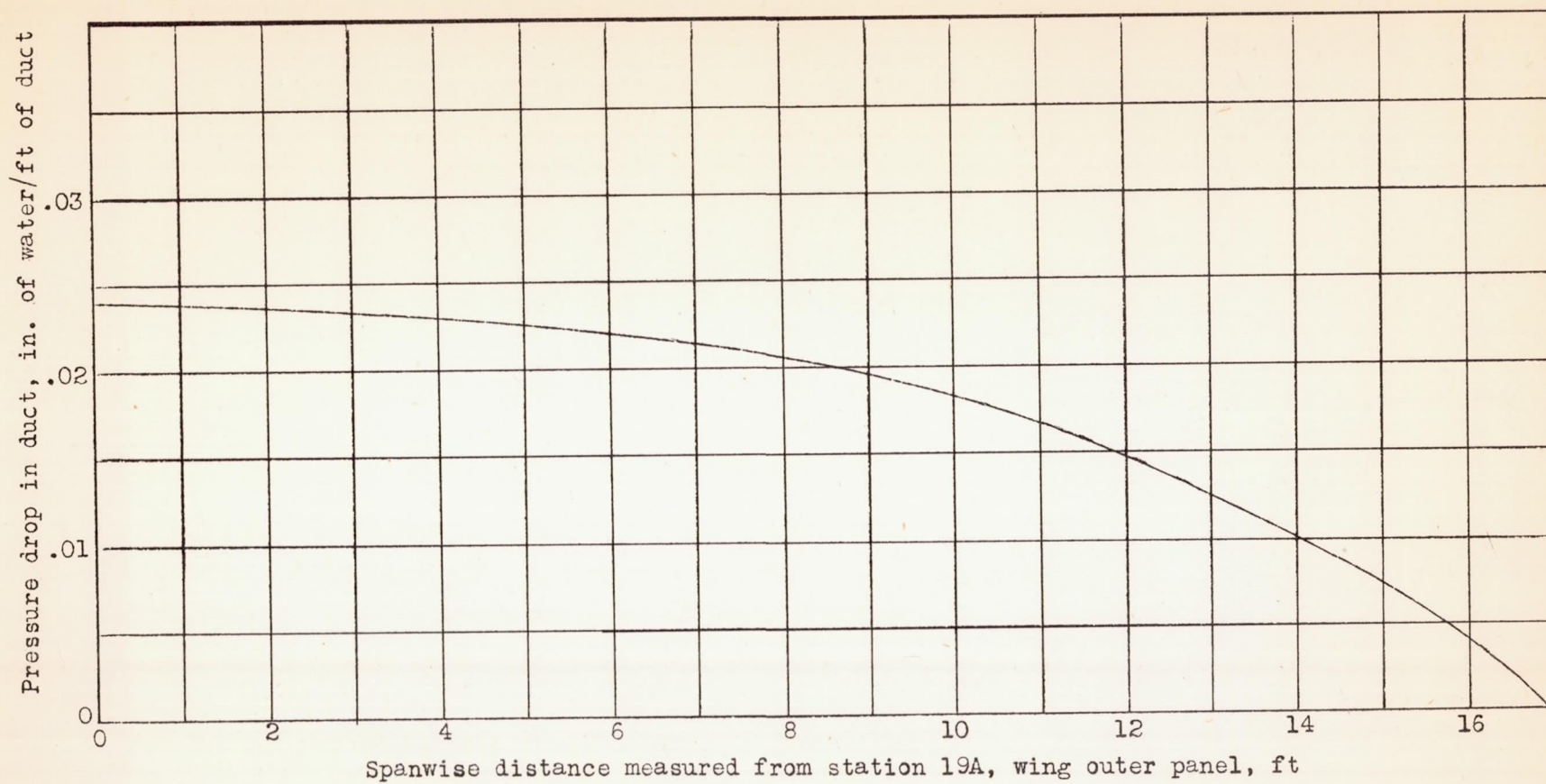


Figure 31.- Pressure drop in wing outer panel duct, B-17F airplane.

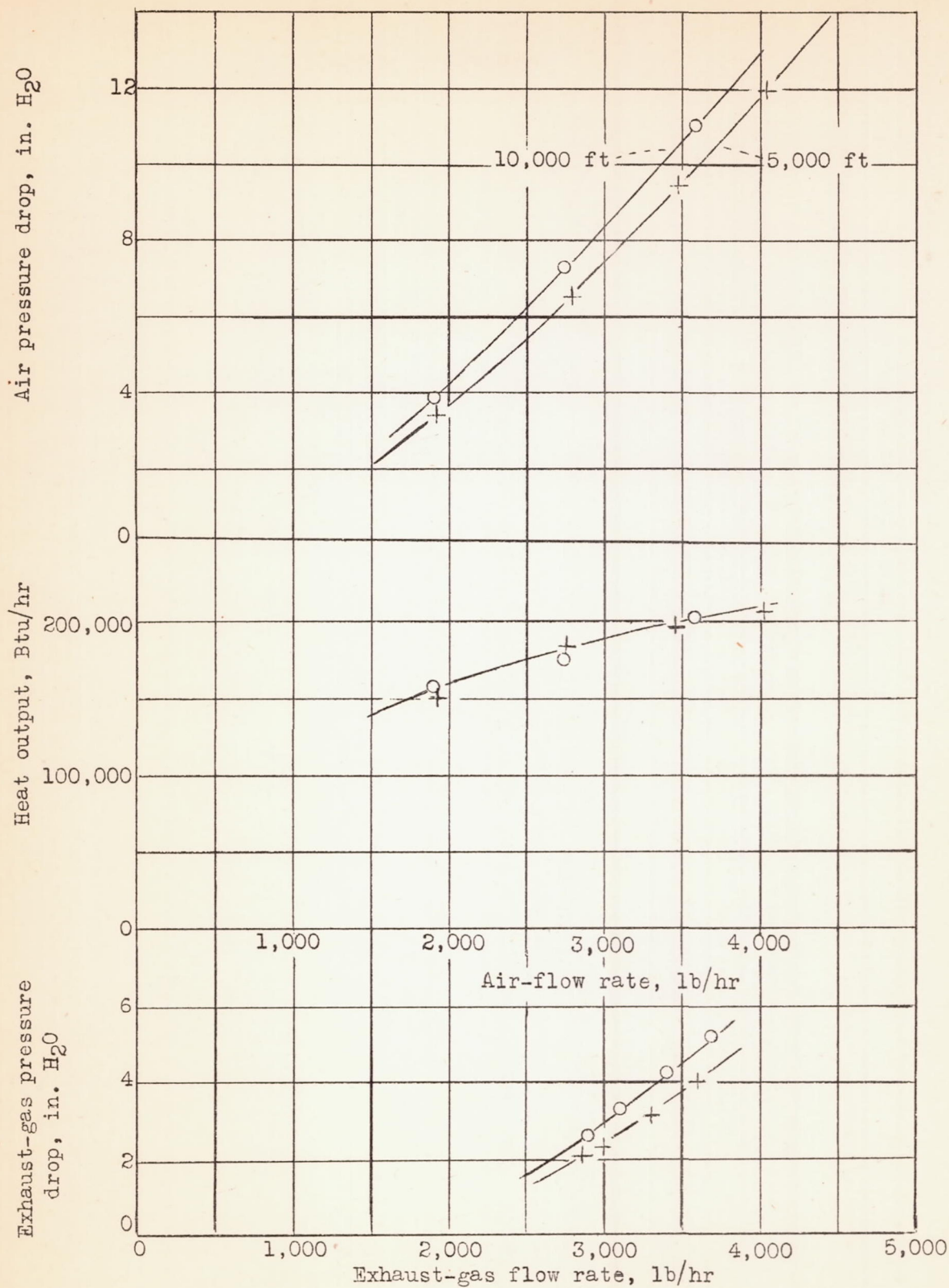


Figure 32.- Flight test data for B-17F right-inboard heat exchanger installed on single-engine test airplane.

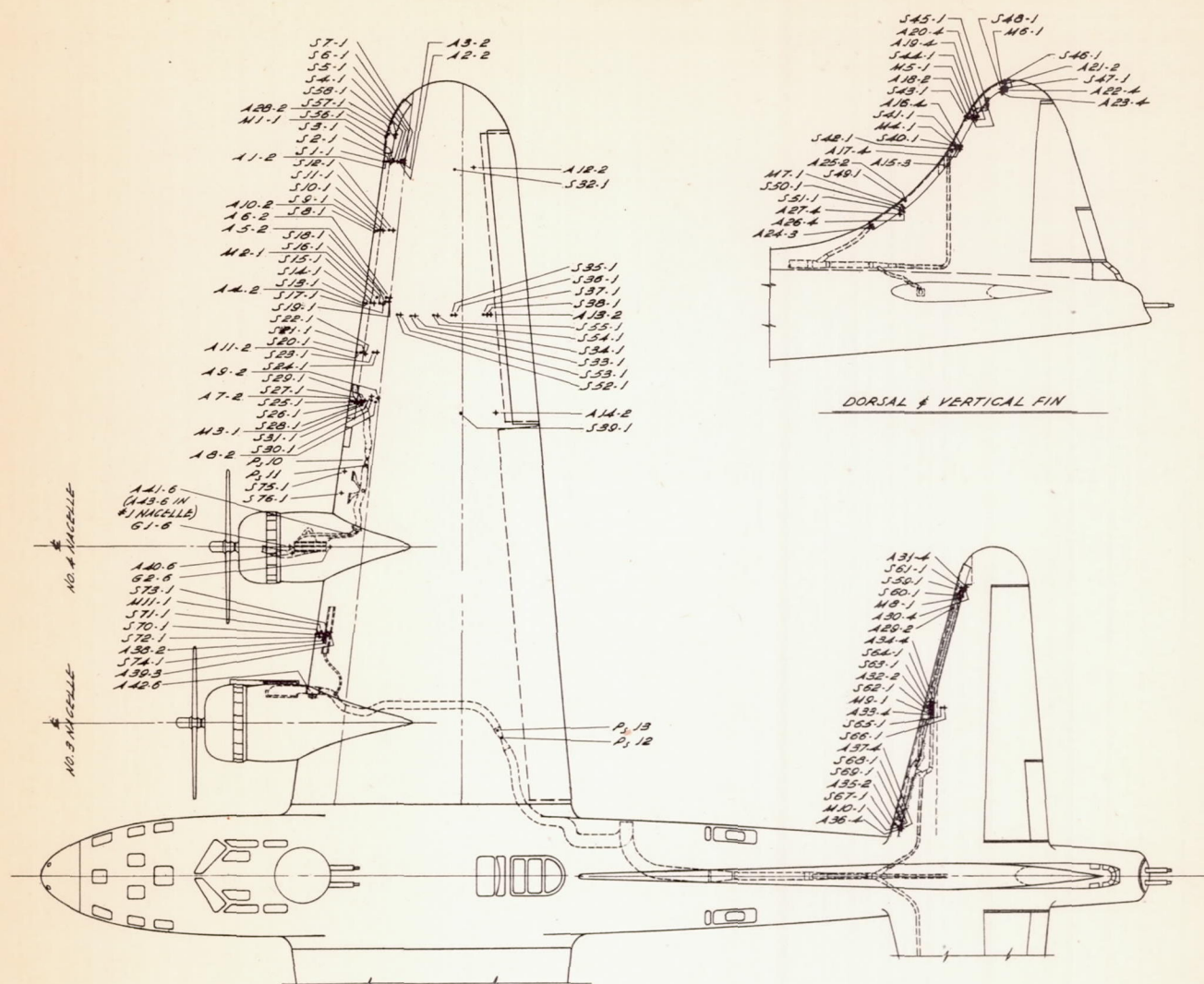
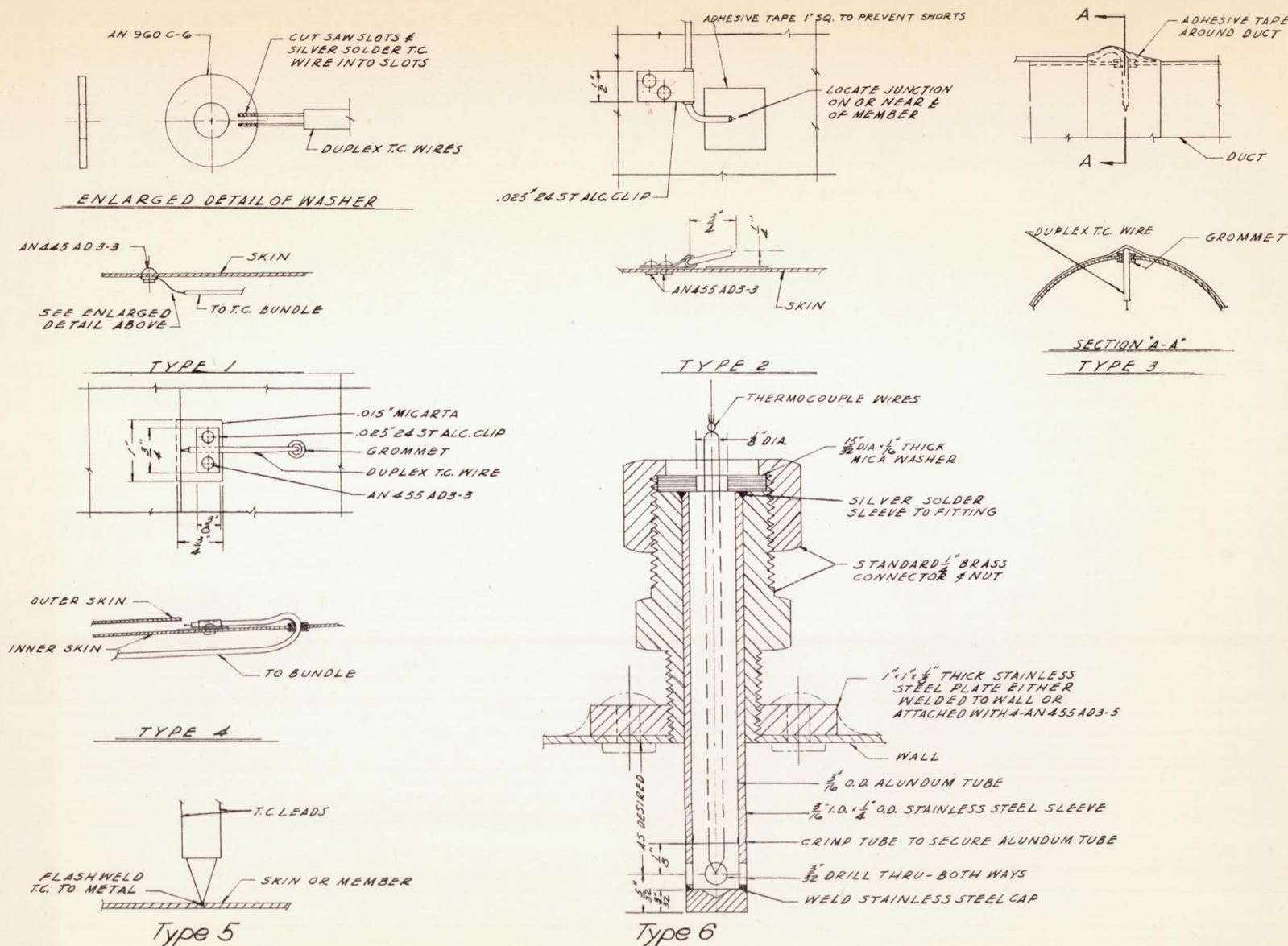


Figure 33.— Location of thermocouples and pressure orifices for testing performance of B-17F thermal ice-prevention system.



Typical thermocouple mounting details - Not to scale
Figure 34.- Thermocouple types employed in tests of B-17F thermal ice-prevention system.